



Evolution and biogeography of *Memecylon*

Prabha Amarasinghe^{1,2,3,11} , Sneha Joshi⁴, Navendu Page⁵, Lahiru S. Wijedasa^{6,7}, Mary Merello⁸, Hashendra Kathriarachchi⁹, Robert Douglas Stone¹⁰ , Walter Judd^{1,2}, Ullasa Kodandaramaiah⁴ , and Nico Cellinese^{2,3} 

Manuscript received 6 July 2020; revision accepted 2 December 2020.

¹ Department of Biology, University of Florida, Gainesville, Florida 32611, USA

² Florida Museum of Natural History, University of Florida, Gainesville, Florida 32611, USA

³ Biodiversity Institute, University of Florida, Gainesville, Florida 32611, USA

⁴ Indian Institute of Science Education and Research, Thiruvananthapuram, India

⁵ Wildlife Institute of India, Dehradun, India

⁶ Integrated Tropical Peat Research Program, NUS Environmental Research Institute (NERI), National University of Singapore, Singapore 117411

⁷ ConservationLinks Pvt. Ltd., 100 Commonwealth Crescent, no. 08-80, Singapore, 140100

⁸ Missouri Botanical Garden, St. Louis, MO, USA

⁹ Department of Plant Sciences, University of Colombo, Colombo, Sri Lanka

¹⁰ School of Life Sciences, University of KwaZulu-Natal, South Africa

¹¹ Author for correspondence (e-mail: praagri@gmail.com)

Citation: Amarasinghe, P., S. Joshi, N. Page, L. S. Wijedasa, M. Merello, H. Kathriarachchi, R. D. Stone, et al. 2021. Evolution and biogeography of *Memecylon*. *American Journal of Botany* 108(3): 1–19.

doi:10.1002/ajb2.1624

PREMISE: The woody plant group *Memecylon* (Melastomataceae) is a large clade occupying diverse forest habitats in the Old World tropics and exhibiting high regional endemism. Its phylogenetic relationships have been previously studied using ribosomal DNA with extensive sampling from Africa and Madagascar. However, divergence times, biogeography, and character evolution of *Memecylon* remain uninvestigated. We present a phylogenomic analysis of *Memecylon* to provide a broad evolutionary perspective of this clade.

METHODS: One hundred supercontigs of 67 *Memecylon* taxa were harvested from target enrichment. The data were subjected to coalescent and concatenated phylogenetic analyses. A timeline was provided for *Memecylon* evolution using fossils and secondary calibration. The calibrated *Memecylon* phylogeny was used to elucidate its biogeography and ancestral character states.

RESULTS: Relationships recovered by the phylogenomic analyses are strongly supported in both maximum likelihood and coalescent-based species trees. *Memecylon* is inferred to have originated in Africa in the Eocene and subsequently dispersed predominantly eastward via long-distance dispersal (LDD), although a reverse dispersal from South Asia westward to the Seychelles was postulated. Morphological data exhibited high levels of homoplasy, but also showed that several vegetative and reproductive characters were phylogenetically informative.

CONCLUSIONS: The current distribution of *Memecylon* appears to be the result of multiple ancestral LDD events. Our results demonstrate the importance of the combined effect of geographic and paleoclimatic factors in shaping the distribution of this group in the Old World tropics. *Memecylon* includes a number of evolutionarily derived morphological features that contribute to diversity within the clade.

KEY WORDS biogeography; character evolution; divergence times; Melastomataceae; *Memecylon*; phylogenomics.

Tropical plants that form large clades and occupy wide distribution ranges have long been of interest to scientists (Corner, 1964; Nepokroeff et al., 1999; Goldenberg et al., 2008; Moonlight et al., 2018; Gamisch and Comes, 2019). *Memecylon* (Melastomataceae) is a large clade (>350 species) of woody plants that has diversified across the Old World tropics (Maxwell, 1980; Bremer, 1988; Renner et al., 2007; Stone, 2014) and, therefore, offers opportunities to understand the historical factors responsible for the current distribution and assembly of Paleotropical forests. This group is found in diverse forested habitats and covers a vast geographic range spanning tropical Africa, Madagascar and other islands of the western Indian Ocean, South Asia, Southeast Asia, and the southwestern

Pacific islands, with an easternmost limit in Tonga (Maxwell, 1980; Bremer, 1988; Bowman, 1992; Stone, 2014). A notable biogeographic feature of *Memecylon* is that only a few taxa are widely distributed (e.g., *M. ovatum* Sm.), while others exhibit high regional or local endemism (Stone, 2012, 2014). For example, 14 of the 32 presently known species in Sri Lanka are endemics (Bremer, 1988), and remarkable endemism is also seen in Madagascar (96/96) and India (21/49) (Stone, 2012, 2020; Das Das et al., 2015). The vegetative and reproductive characters of *Memecylon* are distinctive compared to other members of Melastomataceae (Bremer, 1979, 1988; Maxwell, 1980; Stone, 2006, 2012, 2014), such that some workers have segregated this group (also including *Mouriri*, *Votomita*, *Spathandra*,

Lijndenia, and *Warneckea*) as subfamily Olisbeoideae (e.g., Stone, 2006) or into its own family, the Memecylaceae (e.g., Renner, 1993; Clausen and Renner, 2001). Previous studies and taxonomic treatments suggested that *Memecylon* does not exhibit high morphological character variations (Maxwell, 1980; Stone, 2006, 2014), although character evolution has not been thoroughly investigated.

An earlier phylogenetic study of this group was based on maximum likelihood (ML) analyses of the internal and 5' external transcribed spacers (ITS, ETS) of the nuclear 18S–26S ribosomal DNA (rDNA) cistron, with extensive taxon sampling from Africa, Madagascar, and other islands of the western Indian Ocean (Stone, 2014). *Memecylon* was shown to be monophyletic, and subclade *Mouririoidae* (i.e., a *Memecylon* group strictly from western and central Africa) was recovered as sister to the rest of *Memecylon* (Stone, 2014), while other geographically based subclades were named after the regions where they occur, such as east African, western and central African, Malagasy (including the neighboring islands of Mauritius, Réunion, and Mayotte), Indo–Malaysian, Southeast Asian, and Seychelles–Sri Lankan clades. The east African clade includes the *Buxifolia* subclade that also occurs in Madagascar (Stone, 2014).

Although phylogenetic relationships of African–Malagasy *Memecylon* have been studied (Stone, 2014), additional data are needed to increase the resolution and support among several major clades. Moreover, previous analyses had only limited taxon sampling from the Asia–Pacific region, despite the fact that this area harbors ~50% of the total *Memecylon* diversity (Renner et al., 2007), which is also highlighted by its economic importance for medicinal, timber, and fiber values (Jin et al., 2013; Tanaka–Oda et al., 2015; Bharathi et al., 2016). However, including taxa from these areas is challenging because many *Memecylon* species are endemic and/or rare, and difficulties in obtaining permits for collection and export have precluded a comprehensive and/or high-density sampling.

Memecylon is a difficult group for systematics and phylogenomic studies due to sterile individuals frequently found in the field and problems in DNA sequencing. Repeated extractions, purification, and/or sequencing are necessary for the application of next-generation sequencing (NGS) methods (Jantzen et al., 2020). Identification of herbarium vouchers is challenging due to little variation in floral characters, seasonal flowering, and/or rarity of flowering events (Stone, 2014). Furthermore, identification of *Memecylon* using herbarium collections is difficult due to changes in the appearance of preserved material, and flowers and fruits are rarely found together on the same specimen. For these reasons, a comprehensive assessment of the evolution of *Memecylon* is still needed.

Age estimation of *Memecylon* and its individual lineages is important to uncover the biogeographic history of this group and to understand the historical processes responsible for its widespread distribution in the Old World tropics. However, divergence time and biogeographic analyses of *Memecylon* have not been published to date, although previous studies have approximated the time of origin of *Memecylon* within the context of the larger Melastomataceae and Myrtales clades (Renner et al., 2001; Morley and Dick, 2003; Renner, 2004; Berger et al., 2016; Veranso–Libalah et al., 2018). In these studies, Olisbeoideae were represented by only a few samples of *Memecylon* and *Mouriri*. A broader taxon sampling from the entire distributional range of *Memecylon* is required to gain more precise internal age estimates and a full understanding of the biogeographic history of this group.

Studies involving reconstruction of ancestral traits and of the evolutionary forces driving character evolution of *Memecylon* are

lacking to date. Characters considered to be diagnostic have included size and shape of leaves, leaf venation, inflorescence position, dimensions of hypantho–calyx, color of petals, presence of lipid-secreting glands on anther connectives, and other vegetative and reproductive traits (Jacques–Félix, 1978; Bremer, 1983, 1988; Maxwell, 1980; Stone et al., 2006, 2008; Stone, 2012, 2014). These treatments have shown that floral characters are highly conserved in the group and that *Memecylon* taxa generally cannot be diagnosed by a single morphological character; rather, various characteristics must be used in combination (Maxwell, 1980). However, when studying herbarium specimens, it is clear that within the *Memecylon* clade there is considerable vegetative and reproductive trait heterogeneity, which is worth investigating in a phylogenetic context.

Multiple, rapidly evolving low-copy nuclear (LCN) markers, which are also characterized by independent and biparental inheritance, are useful for accurately reconstructing phylogenies (Sang, 2002). Therefore, we designed probes to target the exons of LCN loci of *Memecylon* (Jantzen et al., 2020). First, we increased *Memecylon* sampling from areas in which its representation was limited in past investigations (i.e., South Asia, Southeast Asia, and the Pacific regions); second, we used our newly generated molecular data to conduct a phylogenomic analysis. Regardless of the many challenges that *Memecylon* poses, with these improvements, we aimed at advancing our knowledge of *Memecylon* evolution by (1) reconstructing phylogenetic relationships at a global scale to understand better the relationships among major lineages; (2) estimating the ages of the major lineages; (3) developing a biogeographic hypothesis for the processes that led to the current pattern of *Memecylon* distribution; and (4) exploring the ancestral character states and inferring plausible ecological and evolutionary factors that may have resulted in these traits.

MATERIALS AND METHODS

Taxon sampling

Silica-dried tissue samples of *Memecylon* were collected in the field, mainly from Sri Lanka, India, Singapore, Thailand, Philippines, Indonesia, Seychelles, Madagascar, and South Africa (Appendix 1), and voucher specimens were deposited at one or more of the following herbaria: BKF, BNRH, BO, CAS, FLAS, FRLH, JCB, MH, NU, PDA, PSU, SEY, SING, and WII (herbarium acronyms: Thiers, 2020). Additional samples of *Memecylon* and an outgroup, *Mouriri*, were taken from herbarium specimens (CAS, FLAS, MO, NY, NSW, and US; see Appendix 1). Plants and their habitats were also photographed, and GPS and ecological data were recorded in the field. One sample per species was selected for the phylogenomic analysis. This included 67 species representing different geographic areas (Africa; Madagascar and other islands of the western Indian Ocean; South Asia; Southeast Asia including Andaman islands and the region west of the Wallace's Line; and Pacific regions east of the Wallace's Line, including northern Australia and the islands of Papua New Guinea, Indonesia, and Philippines).

Library preparation, sequence cleaning, and assembly

To facilitate probe design, genome-skimming data sets were constructed for two distantly related species, *Memecylon dasyanthum* Gilg & Ledermann ex Engl. (this specimen was

determined as *Memecylon afzelii* G. Don in Jantzen et al., (2020) and *M. torricellense* Lauterb., from herbarium collections (MO). Target capture was employed to enrich genomic regions of interest for the rest of the samples. All accessions were processed according to a workflow described in detail in Jantzen et al. (2020) and summarized here. Total genomic DNA was extracted following a modified CTAB extraction protocol (Jantzen et al., 2020). DNA was quantified using a Qubit DNA BR assay (Thermo Fisher Scientific, Waltham, Massachusetts, USA), and quality was evaluated using both Nanodrop 2000 (Thermo Fisher Scientific, Waltham, Massachusetts, USA) and gel electrophoresis. Preparation and quantification of double-barcoded genomic libraries and target enrichment were performed by RAPiD Genomics (Gainesville, Florida, USA; <http://www.rapid-genomics.com>) using a customized probe set for two distantly related clades of Melastomataceae (Jantzen et al., 2020). Cleaned target-capture reads were assembled with the Burrows-Wheeler alignment version of HybPiper version 1.3.1 using the template sequences used for probe design as references (Johnson et al., 2016). Genome skims were assembled using a modified HybPiper script. First, the exons were retrieved using a HybPiper script. Then the post-processing scripts in the HybPiper were used to retrieve intron regions flanking targeted exons and the supercontigs (Johnson et al., 2016). The retrieved supercontigs were used for phylogenetic analyses. The post-processing HybPiper script “paralog_investigator.py” (Johnson et al., 2016) was used to extract coding sequences from alternative contigs flagged by the program. This HybPiper script identifies paralogs, which are indicated by the presence of multiple long contigs for a locus (Johnson et al., 2016). The identified paralogs were removed from the analysis.

Phylogenetic analyses

The supercontigs were individually aligned using MAFFT version 7.215, with the default gap opening penalty and -auto option which automatically selects an appropriate strategy from L-INS-i, FFT-NS-I and FFT-NS-2 algorithms according to data sizes (Katoh and Standley, 2013).

The alignments were trimmed using trimAl version 1.2 (Capella-Gutiérrez et al., 2009) with a gap score of 0.9. All alignments were reviewed using Geneious version 10.2 (Kearse et al., 2012) and evaluated for sequence length, missing data, and quality of alignment. Short sequences that were not retained after trimAl step, and poor-quality alignments, were removed. Gene trees were generated for each of the individual gene alignments using ML analysis performed with RAxML version 8.2.12 (Stamatakis, 2014), assuming a GTRGAMMA model and with 500 rapid bootstrap (BS) pseudoreplicates. Here, a bootstrap search for each gene was performed and the optimal tree for the original matrix was inferred. The gene trees were manually reviewed, and uninformative genes were removed on the basis of the topologies inferred from ML analysis. These uninformative genes included genes that have no variation and genes that have resulted in trees with no resolution. The remaining genes (i.e., 100 supercontigs) were concatenated, and a partition scheme was provided using Phyx version 8.2.0 (Brown et al., 2017). ML analysis was performed following the above RAxML parameters for the concatenated data set, with the exception of using 100 bootstrap pseudoreplicates.

To infer a coalescent species tree, the 100 optimal gene trees generated from RAxML were input to ASTRAL-III version 5.0.3 (Zhang et al., 2018). Topological comparisons between the concatenated and coalescent species trees were performed using the “cophylo” function of the R package phytools version 0.6.4.4 (Revell, 2012). The gene trees were rooted with the outgroup using Phyx and were then input to PhyParts, a program that calculates the proportion of unique, conflicting, and concordant nodes between gene trees and a reference tree (Smith et al., 2015). Here, PhyParts assessed the congruence of individual gene trees with the ASTRAL-III species tree. Additionally, we used RAxML to optimize branch lengths on the ASTRAL-III topology as measured in the per site substitution rate. The branch lengths of ASTRAL-III represent the amount of coalescence, which is useful for understanding discordance but cannot be used for biogeographic or ancestral state reconstruction analyses. Because informative branch lengths are required for downstream analyses, the resulting ASTRAL-III topology was constrained on the ML analysis. Statistical support was defined for the resulting species trees as follows: for the BS support on the ML trees, we consider strong support as $BS \geq 95$, moderate support as $95 > BS \geq 60$, and poor support as $BS < 60$; and for local posterior probability (PP) values on ASTRAL-III topology, we consider strong support as $PP \geq 0.95$, moderate support as $0.95 > PP \geq 0.6$, and poor support as $PP < 0.6$. We present PP values here, because it has been shown that the PP values of clade support have more precision than multilocus bootstrapping (Sayyari and Mirarab, 2016).

Because some samples showed long branches on the concatenated ML tree, RogueNaRok version 1 (Aberer et al., 2013) was used to identify their “rogue taxa” status (i.e., taxa with inconsistent and contradictory phylogenetic placement). Additionally, quartet sampling (QS), a statistical approach that estimates the number of alternative topologies that a resampled quartet tree recovers, was implemented to reassess these samples for “rogue taxa” with the quartet fidelity (QF) scores (Pease et al., 2018) in both ML and ASTRAL-III topologies. Furthermore, quartet concordance (QC), quartet differential (QD), and quartet informativeness (QI) scores at each node from QS analysis were used to understand the informativeness and concordance of the resampled quartets with the input topology.

To provide reliable placement of fossils for dating analysis, outgroup taxa from Melastomataceae and Myrtales clades are required. However, these myrtalean outgroups have only a limited number of LCN genes available, preventing their use in the phylogenomic analysis. Therefore, to increase the sampling of both ingroup and outgroup taxa, we used previously published rDNA data available from GenBank (Appendix S1). The rDNA sequences from target capture data in our samples were assembled using HybPiper and aligned with the GenBank data set. This approach extended the data set from 67 to 164 *Memecylon* species and 31 outgroups. Each gene sequence was separately aligned with MAFFT. The alignments were trimmed using trimAl with a gap score of 0.9 and then concatenated via Phyx with the parameters used in the phylogenomic data set. A hybrid phylogenetic-phylogenomic approach, which was implemented with the -g option on the RAxML script (Stamatakis, 2014), resulted in polytomies within the *Memecylon* clade. Therefore, only rDNA sequences of all samples were used to obtain a large ML tree without polytomies using the RAxML parameters for the concatenated supercontig data set.

Molecular dating

Two phylogenetic trees, (1) ML phylogeny generated using rDNA sequence data of *Memecylon* with other Melastomataceae and myrtalean outgroups and (2) ASTRAL-III-constrained ML tree from the supercontig data set, were used for a dated analysis with the following methods.

First, the ML phylogeny constructed with rDNA sequences was time-calibrated in the context of the larger Myrtales clade. The fossil record in *Memecylon* is very poor, and the only accurately identified fossil is *Memecyloxylon germanicum* Gottwald (Gramann et al., 1975; Gottwald, 1992), but its placement is controversial. Therefore, we used two fossils and two secondary calibration points from Berger et al. (2016) as dating constraints to provide a timeline for the rDNA tree. The earliest Melastomataceae leaf fossil *Acrovena laevis* (Hickey, 1977) at 48.6 Ma was used as the minimum age to constrain the crown of Melastomatoideae. The second fossil is a Melastomataceae seed (26–23 Ma; Collinson and Pingen, 1992), which was used as the stem age of the Melastomataceae plus Rhexieae clades (Clausing and Renner, 2001; Renner et al., 2001; Rutschmann et al., 2007; Berger et al., 2016; Veranso-Libalah et al., 2018). Moreover, two secondary calibration points were used from Berger et al. (2016). One secondary calibration was used to constrain the age estimate for Melastomataceae crown (the clade that includes both the subclades Melastomatoideae and Olisbeoideae) at 90.7 Ma (95% highest posterior density [HPD]: 98.8–82.4 Ma). An additional secondary calibration was used for the root of the tree as the maximum age of 125 Ma, constrained from an estimate for the Myrtales stem. Divergence times among inferred ancestors were estimated under penalized likelihood with the program treePL (Smith and O'Meara, 2012). To identify the optimal smoothing value in the phylogram, a data-driven cross-validation analysis was conducted using treePL. The optimal smoothing value was found to be 1×10^{-8} , and 100 ML bootstrap phylograms were dated using this value. Tree files from the independent runs were combined after removing 25% of trees as burn-in, and age statistics of internal nodes were summarized from the remaining trees using TreeAnnotator version 1.8.0 (Drummond et al., 2012) to construct the maximum clade credibility chronogram. From this combined tree, node ages and 95% HPD values were obtained.

Secondly, the maximum and minimum ages of the *Memecylon* crown clade were constrained on the ASTRAL-III-constrained ML phylogeny due to low BS support values for the major relationships within the *Memecylon* clade in the rDNA phylogeny. Therefore, we present the molecular dates based on the ASTRAL-III-constrained ML phylogeny. The treePL analysis and construction of a maximum clade credibility chronogram from ML bootstrap phylograms were repeated as above with the exception of providing 1×10^{-9} as the optimal smoothing value found from the analysis.

Biogeographic analysis

Six broad biogeographic areas were defined for the distributions of extant *Memecylon* and outgroups in our data set: (A) North and South America—only for the outgroup; (B) continental Africa; (C) Madagascar and other islands of the western Indian Ocean; (D) South Asia; (E) Southeast Asia, including Andaman islands and the region west of Wallace's Line (between Borneo and Sulawesi); and

(F) Pacific, east of Wallace's Line, including northern Australia, the Philippines, and Papua New Guinea.

Occurrence data for all terminal taxa were collected from Global Biodiversity Information Facility (<http://data.gbif.org/species/>), taxonomic treatments (Bremer, 1979, 1988; Maxwell, 1980; Stone et al., 2006, 2008, 2019; Stone, 2012, 2014), and herbarium specimens. This occurrence data set was manually inspected for identification accuracy and coded for the presence or absence of the entire lineage in the six geographic areas. The ancestral ranges were estimated using the BioGeoBEARS package in R (Matzke, 2013, 2014) for the ASTRAL-III-constrained ML tree dated with TreePL. The maximum number of ancestral areas to be reconstructed at each node was set to five, and in a second approach, it was restricted to two because the age estimates of the nodes did not suggest a wide ancestral distribution. The models tested included DEC, BAYESAREALIKE, and DIVALIKE (Matzke, 2014). The likelihood ratio tests of Akaike's information criterion (AIC) and AIC_c scores were compared to measure the overall model fit to the data. Additionally, DEC+J, which accounts for founder-event speciation, was applied independently from the test, due to criticisms regarding the inappropriate statistical comparison between models with and without +J (Ree and Sanmartín, 2018). The probabilities of ancestral areas were estimated using the probability range script (Matzke, 2014).

Character evolution

A total of 25 discrete and continuous characters were scored for *Memecylon* species. Characters, and character state definitions and methods of scoring, are presented in Appendix S2. Many of these characters have previously been considered taxonomically useful; however, number of flowers per axis, number of internodes per floral axis, and number of bracts per branch of the inflorescence are new characters examined in this study and had not been investigated for their utility in diagnosing clades. A character matrix was constructed for ingroup species and the outgroup, *Mouriri*, by direct examination of herbarium material and digitized specimens, observations in the field and inspection of photographs, and/or available literature from species descriptions and taxonomic revisions (Appendix S3).

The following criteria were used for coding characters in discrete states for ML analysis: *Memecylon* species were considered the operational taxonomic units (OTUs) in the matrix. For continuous characters, the total range of variation was used as maximum and minimum values (Appendix S2). Continuous characters were included only for leaf length, leaf width, peduncle length, pedicel length, and calyx-lobe length. Measurements of some of these characters were directly obtained from species descriptions and the taxonomic treatments listed above, and some were measured from the digitized and scaled herbarium material using ImageJ version 2 (Rueden et al., 2017). Continuous characters were plotted using the package ggplot2 (Wickham, 2016) in R version 3.6.1 (R Core Team, 2019) to visualize their variation. These continuous characters were converted to discrete characters based on assigned cutoff values on the graphs. The cutoff values were determined using the significantly large gaps in the distribution of the values on the graphs. Characters with >50% missing data among the *Memecylon* species sampled in this study were discarded. Many qualitative characters were found to have overlapping ranges between species,

and accordingly were not selected for character mapping, due to difficulties in coding the pattern of variation as discrete character states. Morphological characters were not included if they were potentially subject to phenotypic plasticity or if coding was deemed too subjective.

The coded morphological characters were analyzed with the dated ASTRAL-III-constrained ML phylogeny of *Memecylon*. Ancestral character states were reconstructed with joint likelihoods as implemented in R with phytools and APE version 5.1 (Paradis et al., 2004). The equal-rates (ER) model (equal forward and reverse transitions between states) and the all-rates-different (ARD) model (all possible transitions between states) were tested to select the appropriate rate-model for the analysis. The lambda parameter (Pagel, 1999) and likelihood ratio values were used to compare the two models.

RESULTS

Phylogenetic analyses

Removal of paralogs, low-quality alignments, and uninformative genes resulted in 100 phylogenetically informative supercontig alignments out of 291 loci targeted for *Memecylon*. One hundred and fifteen loci were duplicates of the template sequences used for probe design (Jantzen et al., 2020) and were not used for the assembly. Forty-five sequences were identified as paralogs from paralog retrieve scripts. For the genes discarded due to lack of information, 25 were Melastomataceae specific and six were from the Angiosperms353 probe set (Johnson et al., 2019). Of the 100 supercontigs used, 90 were Melastomataceae specific and 10 were from the Angiosperms353 probe set. In these individual supercontig alignments, the minimum taxon coverage for a gene retained for the analysis was 11. Summary statistics for the alignments of the supercontigs, introns, and exons (alignment length, variable sites, constant sites, phylogenetically informative sites, and proportion of missing data) are presented in Table 1. Probe name, number of samples per sequence, total sites, phylogenetically informative sites, invariant sites, and constant sites for individual genes are provided in Appendix S4. The total length of the trimmed and concatenated supercontig alignment of 68 samples was 62,100 bp. In the alignment, the sequences of *M. fruticosum* King, *M. elaeagni* Blume, *M. lateriflorum* (G. Don) Bremek., *M. lanceolatum* Blanco, *M. magnifoliatum* A. Fern. & R. Fern., and *M. symplociforme* Merr. were problematic because each contained a significant amount of missing data (53.9%, 66.6%, 97.9%, 79.6%, 99.3%, and 77.5%, respectively) due to low success in target capture for these samples. However, these samples were retained in the analysis, because some of them showed important relationships in the resulting phylogeny (e.g., sister relationship of *M. lateriflorum* to the rest of the *Memecylon* clade).

TABLE 1. Variation statistics for alignments from the recovered sequences. Total number of genes are 100 for exons, introns, and supercontigs.

Parameters	Exons	Introns	Supercontigs
Alignment length (bp)	39,733	21,370	62,100
Parsimony-informative sites	4066	5885	9573
Variable sites (bp)	10,525	14,025	23,633
Constant sites (bp)	29,423	8466	37,369
Missing data (%)	10.4	14.6	11.9

The ML analysis of the concatenated supercontig data set strongly supported most of the nodes (43 out of 67). In general, support values were moderate to high at deeper nodes, and lower at shallower nodes (Appendix S5). In the ML phylogeny, *M. fruticosum* and *M. lanceolatum* showed long branches (Appendix S5). Removing these two species from the data set did not affect the topology; in the QS analysis, their QF values were not significantly low compared to other samples, and RogueNaRok did not identify them as “rogue taxa” (see below). Therefore, we retained them in the phylogenomic analysis.

The coalescent-based analysis using ASTRAL-III recovered nine major lineages within *Memecylon*, reflecting their continental distribution (Fig. 1): African1 (AF1), African2 (AF2), African3 (AF3), African4 (AF4), Malagasy1 (MA1), Malagasy2 (MA2), Southeast Asia (SEA), Pacific (PA), and South Asia consisting of two subclades (SA1 and SA2). Two African lineages, each represented by a single terminal, were related to the rest of the *Memecylon* clade (Fig. 1: AF1 and AF2): one lineage (AF1) consisted of the west–central African *M. lateriflorum* and the other (AF2) contained *M. magnifoliatum* from east Africa. A large clade (A) that included the remaining taxa spanned the entire distribution of *Memecylon*. Within this group, clade B containing *Memecylon* lineages from Africa (Fig. 1: AF3 and AF4) and Madagascar (Fig. 1: MA1 and MA2) was sister to the rest (clade C). The Malagasy lineage (MA2) was sister to AF4. Clade D contained Southeast Asian and Pacific taxa, and Clade E included South Asian *Memecylon*. Within clade D, a Pacific clade (PA) was phylogenetically nested within a Southeast Asian clade (SEA). Lastly, within clade E, subclades SA1 and SA2, which included Sri Lankan and Seychelles taxa, were sister groups.

We found moderate to strong PP support for most nodes (60 out of 67) in the ASTRAL-III phylogeny. For example, *M. lateriflorum* is sister to the rest of *Memecylon* with strong support (PP = 1). The sister group relationship of clade AF2 to clade A was moderately (PP = 0.67) supported. Within the African and Malagasy clade (Fig. 1, clade B), all relationships were moderately to highly supported (PP = 0.73–1.00). In clade B, lineage AF3 from west–central Africa is sister to the clade containing MA1, AF4, and MA2 (PP = 1). The strictly Malagasy (MA2) clade is sister to a clade containing east African (AF4) *Memecylon* (PP = 1). South Asia (Fig. 1) was the largest subclade in terms of sampling, and most of the nodes have high to moderate statistical support, but several (3/33) shallow and deep nodes have low PP support. In the South Asian clade, subclade SA1 consisting of Seychelles (*M. elaeagni*) and Sri Lankan species (*M. rivulare* K. Bremer, *M. rostratum* Thwaites, *M. cuneatum* Thwaites, *M. clarkeanum* Cogn., and *Memecylon* sp. P3) showed moderate support (PP = 0.65) for its relationship to subclade SA2. Andaman *Memecylon* species were included within both South Asian (*Memecylon* sp. 5, *Memecylon* sp. 16, and *Memecylon* sp. 18) and Southeast Asian clades (*Memecylon* sp. 7) with high to moderate PP support (Fig. 1). In the Southeast Asian clade, *Memecylon* sp. 7 from Andaman seemed to be sister to the Southeast Asian and Pacific clade (Fig. 1) with high support (PP = 0.95).

Gene tree and species tree analyses

The coalescent-based analysis using ASTRAL-III recovered relationships that are mostly congruent with those in the concatenated

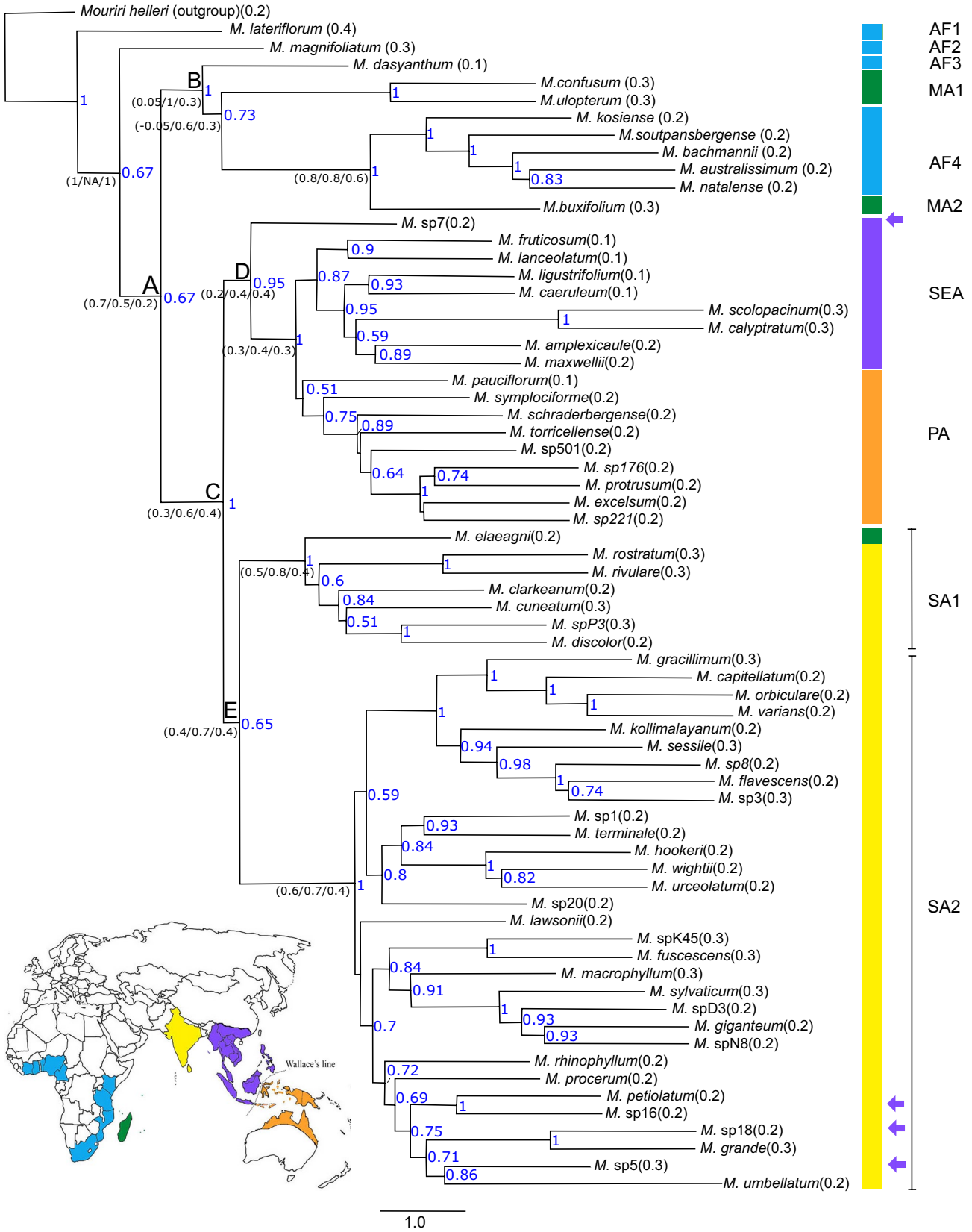


FIGURE 1. ASTRAL-III species tree based on 100 gene trees. Posterior probability (PP) support values are presented in dark blue (PP <0.5 are not shown). Major nodes are labeled A, B, C, D, and E. Scores of quartet concordance (QC)/quartet differential (QD)/quartet informativeness (QI) from quartet sampling are provided only for backbone nodes. Quartet fidelity (QF) scores are given for all tips. Colored bars indicate the geographic regions where the samples were collected corresponding to the map. Purple arrows point to *Memecylon* from Andaman Islands. Nine major lineages are shown: AF1 (African1), AF2 (African2), AF3 (African3), AF4 (African4), MA1 (Malagasy1), MA2 (Malagasy2), South Asia (subclades SA1 and SA2), SEA (Southeast Asia), and PA (Pacific).

ML analysis of the phylogenomic data set. The exceptions were nine taxa (*M. fruticosum*, *M. lanceolatum*, *M. ligustrifolium* Champ. ex Benth., *M. caeruleum* Jack, *Memecylon* sp. 18, *M. procerum* Thwaites, *M. buxifolium* Blume, *M. natalense* Markgr., and *M. bachmannii* Engl.), and their positions were compared using a tanglegram (Appendix S5). The PhyParts analysis (Appendix S6) suggested conflict among gene trees for many relationships within major clades at deeper nodes. The clade containing AF3, MA1, AF4, and MA2 (Appendix S6: B) showed more concordant gene trees in the PhyParts analysis than for the rest of the clades. In the ASTRAL-III analysis, this clade showed a high number of nodes (6/8) with strong PP values (Fig. 1). The PA clade (Appendix S6: E), which contained low to moderate PP support in ASTRAL-III topology (Fig. 1), showed the highest gene tree conflicts compared to the other clades.

The QS, QD, QI, and QF scores for the ASTRAL-III and ML topologies are provided in Figure 1 and Appendix S7, respectively. If QC = 1, this means that all resampled quartets are concordant with the input topology (Pease et al., 2018). In our analysis, one deep node resulted in QC = 1 (Fig. 1: *M. magnifoliatum* to the rest of *Memecylon*). However, QC values for the rest of the deep nodes (except for the MA1 sister relationship with AF4 and MA2) were in the positive range, indicating more concordance of the input topology with the resampled quartet than discordance. QD values indicated a skewed nature of the discordance. QI values for these nodes showed that a moderate proportion (>30%) of replicates were informative. Overall, the results from the QS analysis for deeper nodes suggest that a strong majority of quartets support the focal branches, with discordant skew indicating possible presence of an alternative evolutionary history.

Molecular dating

Divergence age estimates for the clades of interest within *Memecylon* and their respective 95% HPD intervals are presented in Table 2, and these clades are labeled in the chronogram obtained from the treePL analysis (Fig. 2). We estimated the crown age of *Memecylon* to be ~35.0 Ma (95% HPD: 31.9–41.1 Ma) using the dated rDNA phylogeny (Appendix S8). After calibrating this age on the ASTRAL-III-constrained ML phylogeny, the estimated stem age of *Memecylon* was ~44.4 Ma (95%

HPD: 41.6–48.3 Ma) during the Eocene, and the crown age was ~34.3 Ma (95% HPD: 31.9–41.1 Ma), a time between the late Eocene and the early Oligocene (Fig. 2). The split between AF3 and the clade containing MA1, AF4, and MA2 dated back to the Miocene at ~21.3 Ma (95% HPD: 19.1–23.8 Ma). Another major Miocene splitting event between MA2 and AF4 was found at

TABLE 2. Estimated ages (Ma) for the major lineages of *Memecylon* using treePL analysis. Clades are shown in Figure 3.

Clade/lineage	Crown age (95% HPD)	Stem age (95% HPD)
AF1 lineage	–	34.3 (31.9–41.1)
AF2 lineage	–	28.7 (27.5–28.8)
AF3 lineage	–	22.9 (20.7–25.4)
MA1 clade	12.2 (9.6–15.9)	21.3 (19.1–23.8)
AF4 clade	9.8 (7.8–11.6)	12.2 (9.5–14.1)
MA2 lineage	–	12.2 (9.5–14.1)
South Asia clade	21.3 (16.0–24.7)	27.6 (26.8–28.1)
SEA clade	26.7 (25.9–27.3)	27.0 (26.3–27.6)
PA clade	26.6 (25.8–27.2)	27.0 (26.3–27.6)

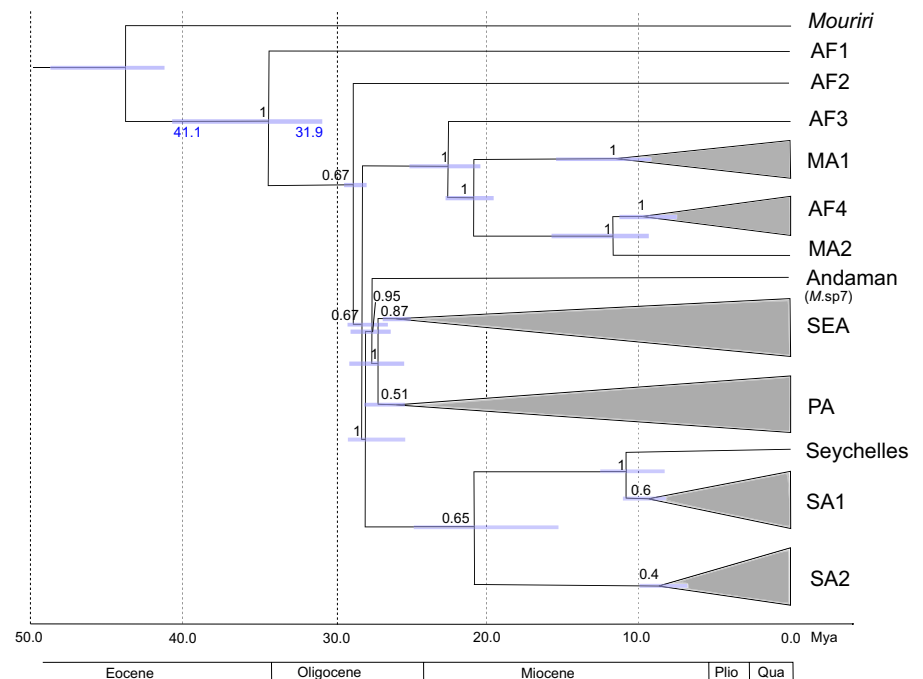


FIGURE 2. Summary chronogram of *Memecylon* from TreePL analysis generated using the ASTRAL-III-constrained RaxML phylogeny. Major clades are AF1 (African1), AF2 (African2), AF3 (African3), AF4 (African4), MA1 (Malagasy1), MA2 (Malagasy2), South Asia (containing subclades SA1 and SA2), SEA (Southeast Asia), and PA (Pacific). Calibration of maximum and minimum ages of *Memecylon* crown are shown in dark blue. RaxML bootstrap (BS) support values are presented in black. Mean divergence time estimates are shown with 95% highest posterior density (HPD: blue bars). Geological epoch abbreviations: Plio = Pliocene; Qua = Quaternary.

~12.2 Ma (95% HPD: 9.5–14.0 Ma). The split between the South Asian clade (SA1, SA2 and Seychelles) and the clade containing SEA and PA was inferred in the Oligocene at ~28.1 Ma (95%

HPD: 26.8–29.1 Ma). The estimated divergence times of the SEA and PA clades were ~27.6 Ma (95% HPD: 26.8–28.1 Ma) and ~27.0 Ma (95% HPD: 26.3–27.6 Ma), respectively.

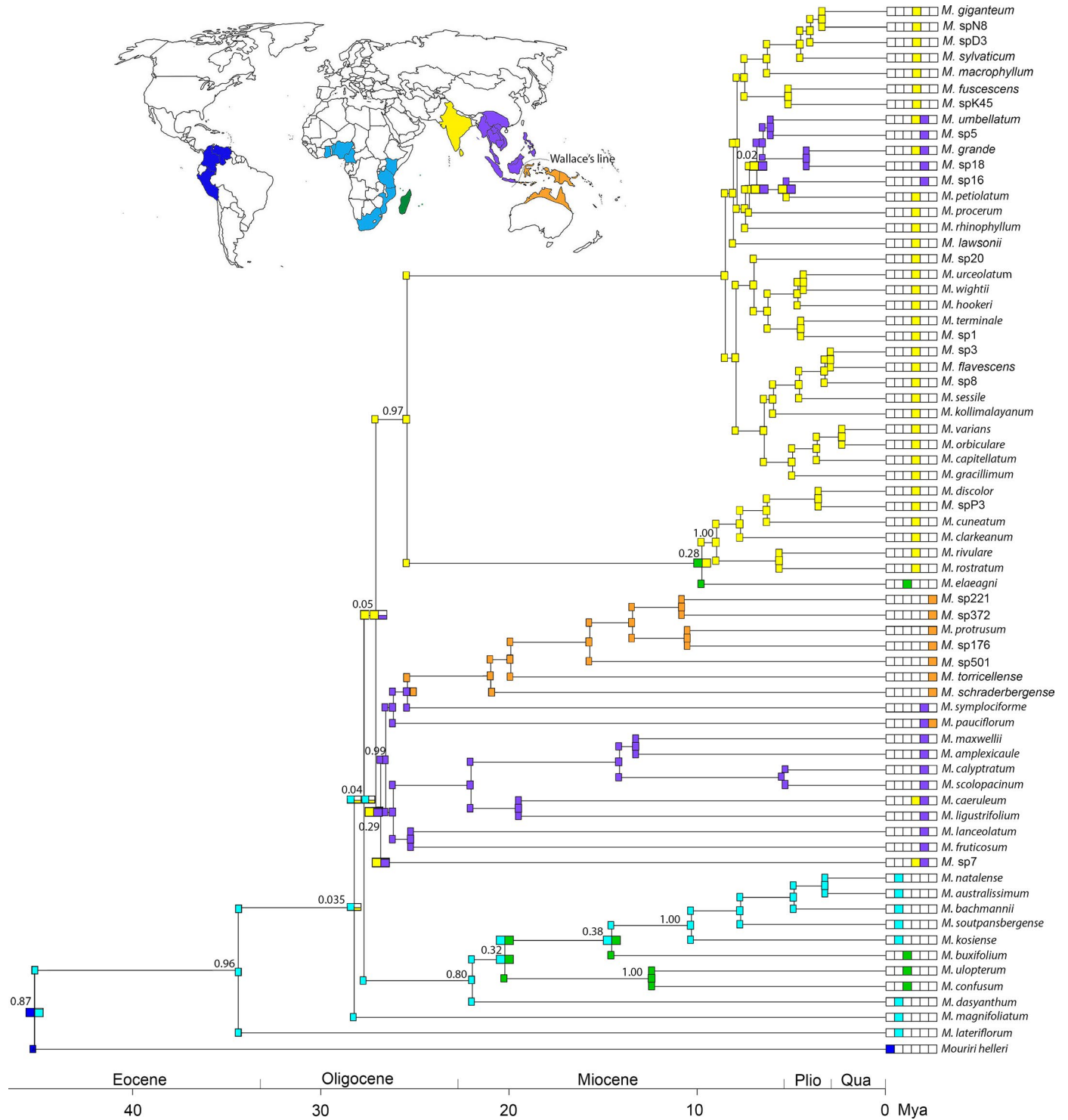


FIGURE 3. Ancestral range estimation of *Memecylon* with BioGeoBEARS (DEC model). The current distribution of each taxon is indicated on the tips of the tree. Geographic areas are color coded as shown in the map; the South American region is only for the outgroup. Probability values for ancestral areas are provided only for the major nodes of interest. Geological epoch abbreviations: Plio = Pliocene; Qua = Quaternary.

Biogeographic analysis

The ancestral areas inferred for internal nodes in the phylogeny are shown in Figure 3. For the ancestral range estimation using BioGeoBEARS, the dispersal-extinction-cladogenesis (DEC) model was identified as the best-fit model. The log-likelihood and AIC score comparison showed the DEC model to be significantly better than the DIVALIKE and BAYESAREALIKE models. The estimate of the range expansion rate parameter (d) was 0.0023, and that of the range extinction rate parameter (e) was $1.0e-12$, indicating that the model relied more on range expansion than on extinction. Summary statistics for all models tested are provided in Table 3. Independent analysis of DEC +J showed the same pattern in the ancestral areas as with the DEC model; however, the per area probabilities for the ancestral ranges were higher in the DEC +J than in the DEC model.

These results indicated that continental Africa was the most likely ancestral area ($p = 0.96$) for *Memecylon* (Fig. 3) and that lineages dispersed into a wide geographic area within mainland Africa, then into Madagascar and Asia. Africa was inferred as the ancestral area ($p = 0.8$) of Malagasy and African *Memecylon* clades (Fig. 3). South Asian *Memecylon* dispersed to Southeast Asia and the Pacific region. A combination of South Asia and Southeast Asia ($p = 0.29$) was inferred as the ancestral area of the Southeast Asian and Pacific *Memecylon* clades.

Character evolution

Six of the 25 morphological characters used for ancestral state reconstruction (Appendix S2) showed unambiguous optimization at the most recent common ancestor of *Memecylon*: shape of twigs, shape of leaves, prominence of leaf veins, inflorescence position, peduncle length, and petal color (Figs. 4 and 5). The other characters were found to have ambiguous optimization because their ancestral states were equally favored. Scoring of these six characters is shown in Appendix S9, and the data matrix for all characters is provided in the Dryad repository. The ARD model was significantly better than the ER model for all six characters (Table 4).

A terete branchlet was inferred as the ancestral state ($p = 0.60$) for the most recent common ancestor of *Memecylon*, with a transition to quadrangular and winged states (Fig. 5A). Based on the present sampling, the winged character state evolved twice as nested in the South Asian clade ($p = 0.98$) and Pacific clade ($p = 0.95$). Clades containing quadrangular twigs might have appeared twice in the evolutionary history of *Memecylon*, once within the African clade ($p = 0.99$), and once in the South Asian clade ($p = 0.95$). Two clades containing terete twigs were found within in the South Asian clade ($p = 0.91$ and 0.67), and another clade containing terete twigs was found in the Southeast Asian clade ($p = 0.70$). All three of

these character states were seen among species of South Asian and Southeast Asian *Memecylon*.

Ovate leaf shape was likely the ancestral state (Fig. 5B: $p = 0.51$). Two large subclades containing *Memecylon* with elliptic leaves were found within South Asian *Memecylon* ($p = 0.96$ and 0.82). Also, subclades containing ovate leaves were found in African ($p = 0.93$), Pacific ($p = 0.89$), and South Asian clades ($p = 0.74$), and these appear to be reversals from derived states. However, there was no *Memecylon* clade containing mainly obovate leaves. Instead, this character state is scattered across clades from different geographic regions.

Among the three states for the vein prominence character (Fig. 4(1)), “indistinct” (Fig. 4(1)A) was favored as ancestral (Fig. 5C: $p = 0.61$). We recovered three clades with distinct veins (Fig. 4(1)C): one in Africa ($p = 0.93$) and two different clades in South Asia ($p = 0.94$ and 0.99). Two clades were found with adaxially impressed veins (Fig. 4(1)B), in the Pacific region ($p = 0.99$) and South Asia ($p = 0.99$). A reversal to indistinct veins was indicated for the Malagasy ($p = 0.51$), South Asian ($p = 0.99$, 0.99 , and 0.97), and Southeast Asian ($p = 0.96$) clades.

Regarding inflorescence position (Fig. 4(2)), an axillary inflorescence (Fig. 4(2)F) was inferred as the ancestral state (Fig. 5D: $p = 0.72$). This character state transitioned to the terminal (Fig. 4(2)E) and cauliflorous (Fig. 4(2)D) positions multiple times. Cauliflorous inflorescences appear to have evolved once within the South Asian ($p = 1.00$) *Memecylon* clade. All African *Memecylon* sampled in this study, except *M. magnifoliatum*, showed axillary inflorescences. The Sri Lankan *Memecylon* clade, which is closely related to *Memecylon* from the Seychelles, showed evolutionary reversal to the axillary state ($p = 0.94$). Southeast Asian *Memecylon* clades showed a diversity of these character states without a particular pattern.

In the reconstruction of peduncle length (Fig. 4(3)), we recovered the short peduncle (Fig. 4(3)I) as the ancestral state (Fig. 5E: $p = 0.60$). Length variation and cutoff values of peduncle lengths are presented in Appendix S10. Six lineages in the phylogeny ($p = 0.66$, 0.63 , 0.97 , 0.63 , 0.64 , and 0.75) shift from short to long peduncles (Fig. 4(3)G). Three clades showed the medium peduncle (Fig. 4(3)H), and they included one clade from each Malagasy ($p = 0.83$), South Asian (0.99), and Pacific ($p = 0.70$) clades.

Blue–purple petal color (Fig. 4(4)K) was inferred as the ancestral state (Fig. 5F: $p = 0.95$) for the most recent common ancestor of *Memecylon*, with a transition to white (Fig. 4(4)J) and pink–red (Fig. 4(4)L). *Memecylon* clades with white petals were recovered from all main geographic regions, including one large clade from Africa ($p = 0.99$) and one small clade each from South Asia ($p = 0.88$), Southeast Asia ($p = 0.97$), Pacific ($p = 0.95$), and Madagascar (0.96). *Memecylon* with blue–purple petals forms a large subclade ($p = 0.97$) within the South Asian clade. A small clade containing pink–red petals was found in South Asian *Memecylon* with a small probability value ($p = 0.15$) to the ancestral node.

TABLE 3. Statistics from ancestral area estimation models in BioGeoBEARS: log-likelihood (LnL); rate of dispersal (d); rate of extinction (e); Akaike’s information criterion (AIC).

Model	LnL	Number of parameters	d	e	AIC
DEC	−72.90	2	0.0026	$1.0e-12$	138.1
DIVALIKE	−75.15	2	0.0032	$1.0e-12$	136.4
BAYAREA	−91.95	2	0.0030	$1.7e-02$	145.0

DISCUSSION

Phylogenetic analyses

Our results for *Memecylon* showed a clear correlation between the topology of the tree and the geographic distribution of species (Fig. 1). This study recovered clades broadly for African–Malagasy, South

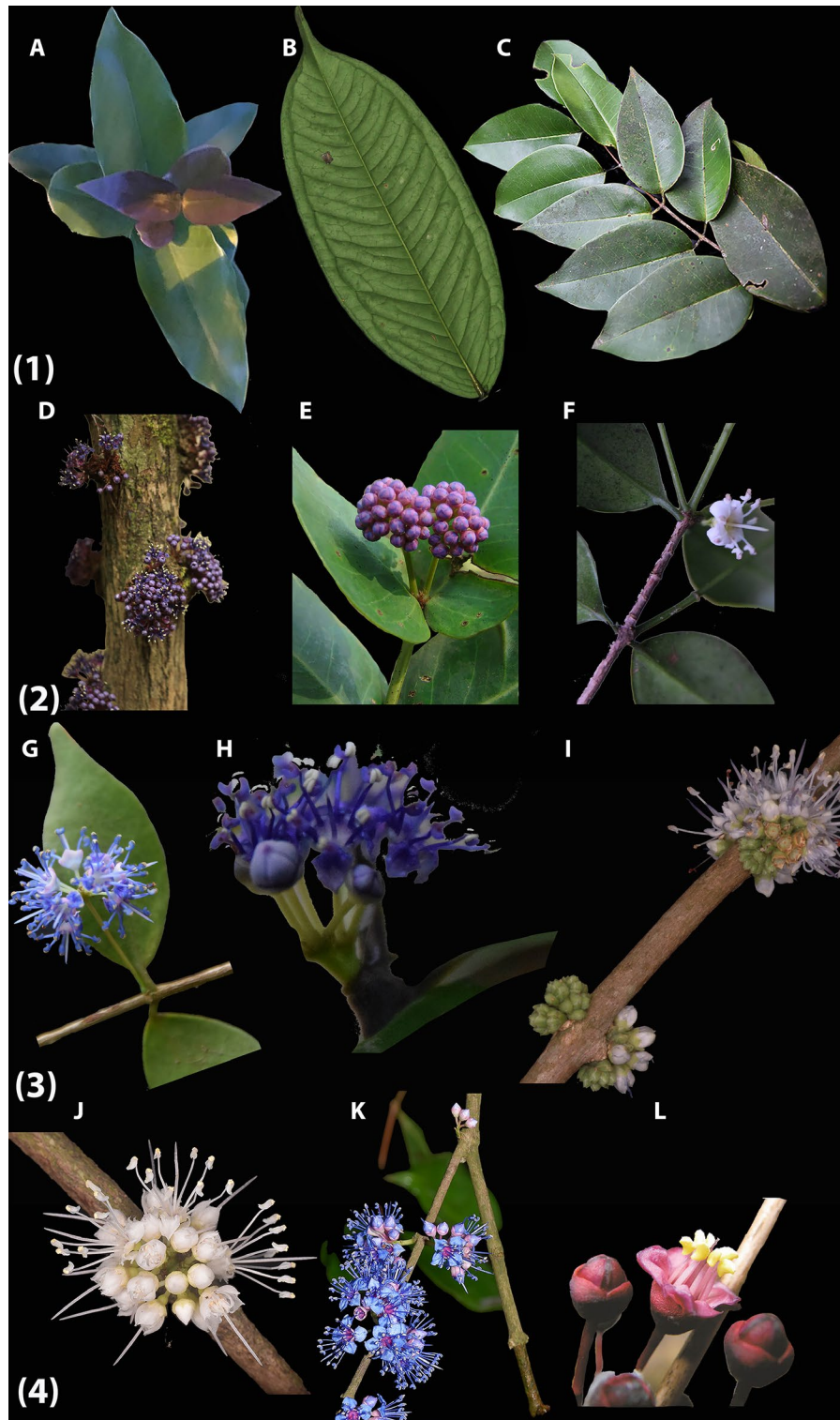


FIGURE 4. Characters of *Memecylon* used for ancestral state reconstruction (four characters out of six are shown here due to unavailability of images of shapes of leaves and cross-sections of stems). (1) Visibility of veins—(A) indistinct: *M. caeruleum* (photo by D. Samanbaddha); (B) adaxially impressed: *M. paniculatum* (photo by R. Lim); (C) distinct: *M. ovatum* (photo by P. Amarasinghe). (2) Inflorescence position—(D) cauliflorous: *Memecylon* sp. (photo by I. Alawatta); (E) terminal: *M. ponmudianum* (source: Sivu et al., 2014); (F) axillary: *M. natalense* (photo by P. Amarasinghe). (3) Peduncle length—(G) long: *M. gracillimum* (photo by P. Amarasinghe); (H) medium: *M. rivulare* (photo by P. Amarasinghe); (I) short: *M. flavescens* (photo by N. Page). (4) Petal color—(D) white: *M. kollimalayanum* (photo by N. Page); (E) blue to purple: *M. umbellatum* (photo by P. Amarasinghe); (F) pink to red: *M. lateriflorum* (source: Stone, 2014).

Asian, and Southeast Asian–Pacific *Memecylon*. Short branches were found within South Asian and Southeast Asian clades in the ML phylogeny, which might be an indication of rapid diversification in these *Memecylon* lineages or, alternatively, could be due to sampling bias. Our PhyParts analysis indicated high gene conflict at shallower nodes, especially in the Southeast Asian clade. Unfortunately, the off-target plastome reads were low (<15%; Jantzen et al., 2020), which precluded a comparative analysis between the nuclear and chloroplast data sets to understand better the nature of discordance.

Our sampling includes a significantly high number of *Memecylon* species (55 out of 67 species used in this study) from Asia and the Pacific and therefore provides insights into the evolution of *Memecylon* in these regions. Within the Asian–Pacific clade (Fig. 1, clade C), Andaman *Memecylon* lineages are phylogenetically nested within either South Asian or Southeast Asian clades. Given that Andaman is geographically in between South and Southeast Asia (Ganeshaiah et al., 2019), this distribution pattern is unsurprising; however, more phylogenetic investigations and biogeographic studies of other plant groups from Andaman, South Asia, and Southeast Asia are needed to explain further the biogeographic patterns of flora in these three regions. Indian and Sri Lankan *Memecylon* are closely related. Additional systematic studies of Sri Lankan, Indian, and Andaman *Memecylon* are highly desirable for understanding better the relationships and taxonomy of the numerous taxa that remain undescribed in these regions.

DNA extraction failures of the samples of *Lijndenia*, *Spathandra*, *Votomita*, and *Warneckea* from herbarium specimens precluded using all known memecyloid outgroups for the phylogenomic analysis. *Mouriri* was the only outgroup sample recovered from our sequencing efforts. Relationships of Olisbeoid outgroups of *Memecylon* were not well supported (Stone, 2014). Therefore, to gain more insights into the relationships between outgroup taxa in Olisbeoideae and *Memecylon*, these samples should be included in future phylogenomic analyses.

Of the nine major lineages identified here, some are congruent with those found in the rDNA study of Stone (2014). For example, the relationships of AF1 and AF2 to the rest of *Memecylon* (Fig. 1) are the same as those found by Stone (2014). However, several other relationships are different. A notable conflict is the placement of the east African clade (Fig. 1: AF4), which is closely related to the clade comprising west-central African and Malagasy (MA1) *Memecylon* in this study. The east African clade is closely related to the Sri Lankan–Seychelles clade in Stone (2014) with weak BS support. Likewise, additional relationships (although poorly supported) differed from those in Stone (2014). For example, the Malaysia–Southeast Asian clade was sister to the clade consisting of east African and Sri Lankan–Seychelles taxa, and an Indo–Malaysian clade was sister to the clade containing other Asian, African, and Malagasy species (Stone, 2014). In this study, geographically adjacent *Memecylon*, such as South Asian and Southeast Asian taxa, and African and Malagasy taxa, are closely related. These relationships support the hypothesis of dispersal within African Malagasy regions first, and subsequently within Asia. Evaluated together, these results provide a more comprehensive scenario regarding the evolutionary history of this plant group.

Origin and biogeography

The estimated ages for the major clades of Melastomataceae are within the ranges obtained in other recent studies that used the

same fossil calibration points but different methodologies (Berger et al., 2016; Veranso-Libalah et al., 2018). For example, the stem age for Olisbeoideae in this study is ~77.1 Ma (95% HPD: 85.9–67.5 Ma; Appendix S8) and lies within the previously estimated time ranges. However, we recover a crown age for *Memecylon* (Fig. 2) that is significantly older than the Miocene crown age from previous studies aimed at estimating divergence times across Myrtales and Melastomataceae (Berger et al., 2016; Veranso-Libalah et al., 2018). The stem age for *Memecylon* is ~44.6 Ma in the Eocene (95% HPD: 36.8–47.3 Ma; Fig. 2), which is consistent with the independently derived age of a wood fossil, *Memecyloxylon germanicum* from the Eocene of western Germany (36.9 (±7) Ma). Although xylem with axially included phloem is a diagnostic characteristic of the *Memecylon* clade (Stone, 2014; Yin et al., 2016), it is also found in *Mouriri* and the other “memecyloid” genera, as well as in *Pternandra* (Van Tieghem, 1891; Van Vliet et al., 1981). Moreover, the usefulness of this wood fossil for dating analysis has been questioned (Renner et al., 2001). Given the low BS values in the rDNA tree (Appendix S11), we estimated divergence times within the *Memecylon* clade based on the dated ASTRAL-III-constrained ML phylogeny (Fig. 2).

Our age estimates for *Memecylon* and its geographically discrete subclades indicate that this lineage is too young for Gondwanan vicariance to have shaped its current distribution pattern. Rather, more recent long-distance dispersal (LDD) events better explain its current distribution in the Old World tropics. The ancestral area reconstruction indicates an African origin of the *Memecylon* stem lineage in the Eocene, with subsequent dispersals to Madagascar and the Asia and Pacific regions (Fig. 3). Interestingly, most *Memecylon* lineages diversified within a geographic region followed by dispersals to other regions. Given that only the Neotropical outgroup *Mouriri* was used as the outgroup, to confirm the African origin of *Memecylon*, all outgroup taxa should be included in the future analyses.

Frugivory by primates and/or birds may have been responsible for transoceanic and terrestrial dispersal of *Memecylon*. A fleshy berry is a character state shared by the whole *Memecylon* clade. These berries are in large clusters, have edible pericarps (Maxwell, 1980), and lack specific adaptations for wind or water dispersal. In South Asia and Southeast Asia, a broad range of frugivores is reported to consume *Memecylon* berries, including birds (e.g., hornbills), mammals (bats, jackals), and reptiles (Gray’s monitor lizard) (Lucas and Corlett, 1998; Swamynathan and Parthasarathy, 2005; Gonzales et al., 2009; Nayak and Davidar, 2010).

Divergence within Africa—Two lineages (Fig. 2: AF1 and AF2) are restricted to mainland Africa. Only one species is sampled for AF1 lineage in this study out of six in Stone (2014). For AF2 lineage, only one species is sampled out of two in Stone (2014). Initially, the AF1 lineage diverged at ~34.3 Ma (95% HPD: 31.9–41.1 Ma) in the Eocene. In Stone (2014), the extant taxa in this lineage are exclusively from western and central Africa and correspond to the *Mouririoidae*. The climate in Africa at that time is presumed to have been warm, wet, and humid to semiarid (Scotese, 2001), and vegetation mainly consisted of diverse lowland forests (Jacobs, 2004; Linder, 2014). Therefore, the most recent common ancestor of *Memecylon* likely lived under humid tropical conditions. Subsequent divergence within Africa presumably gave rise to the AF2 clade. This event seems to date back to the Oligocene at 28.7 Ma (95% HPD: 27.5–28.8 Ma). The AF2 clade comprises *Memecylon* currently restricted to Tanzania in east Africa and corresponding

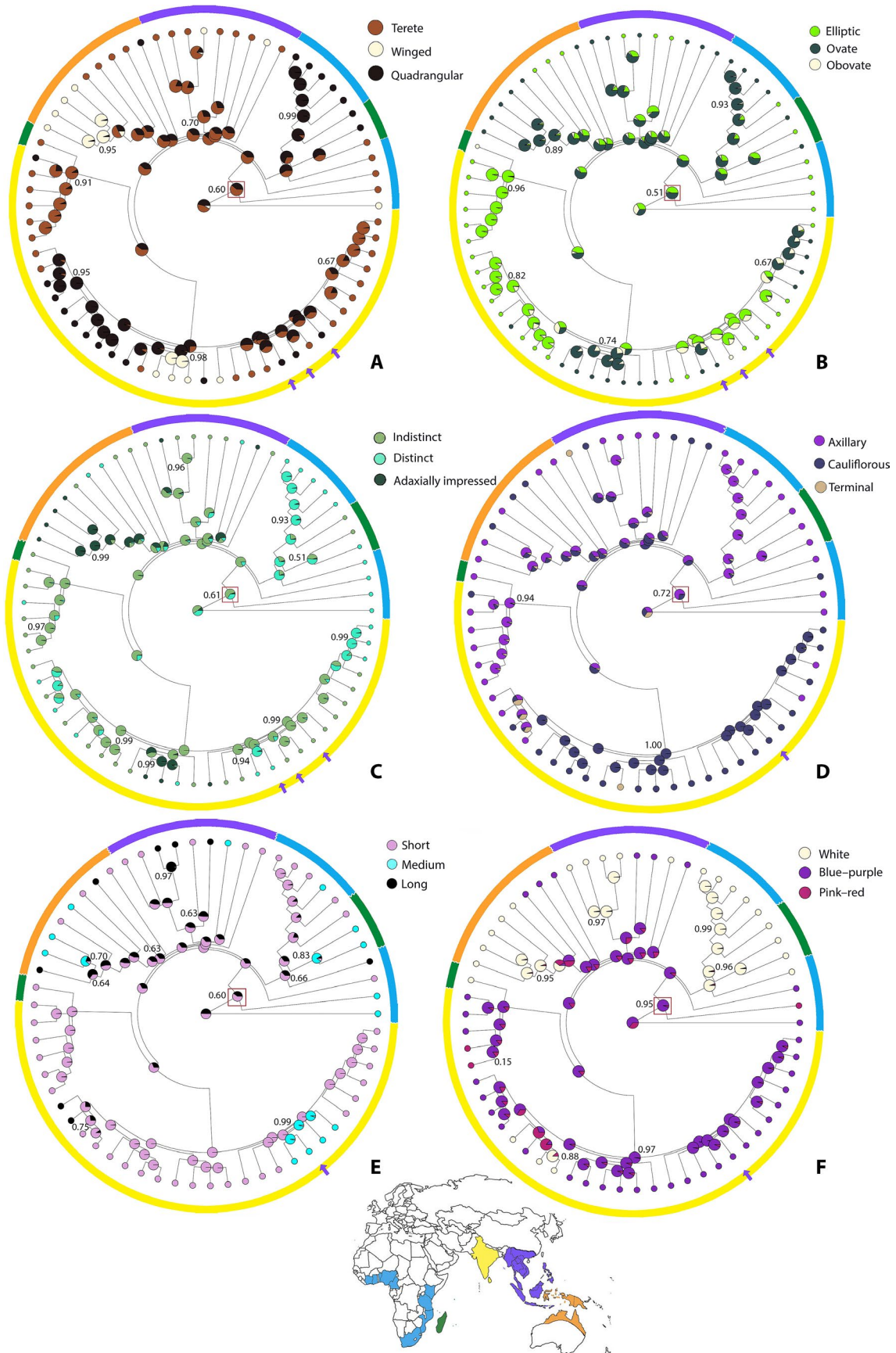


FIGURE 5. Estimation of ancestral character states for (A) twig shape, (B) leaf shape, (C) prominence of veins, (D) inflorescence position, (E) peduncle length, and (F) color of petals. Character states are provided in the key on the top right side for each reconstruction. Pie charts indicate the joint likelihoods of the character reconstruction at that node. Probability values for ancestral nodes are provided for the most recent common ancestor of *Memecylon* and the other ancestors with unambiguous optimizations. Red box highlights ancestral state for each selected character of *Memecylon*. Small circles at the periphery are character states of tips. Colored thick peripheral circles show the geographic regions of the extant taxa as in the map. Purple arrows show *Memecylon* from Andaman.

to *Magnifoliata* in Stone (2014). At that time, eastern and southern Africa contained a mixture of forests and thickets, and forests were dominated by trees and shrubs (Cowling et al., 2005). Therefore, African *Memecylon* that originated in the Eocene may have started expanding its range in the Oligocene from west–central Africa to east Africa through dispersal favored by environmental conditions.

During the Oligocene at 22.9 Ma (95% HPD: 20.7–25.4 Ma), *Memecylon* seems to have dispersed in two different directions (Figs. 2 and 3). One dispersal event was from Africa eastward toward Asia, and another dispersal event led to range expansion within Africa, with subsequent dispersal to Madagascar (Fig. 3). During the time frame of the first dispersal event, the eastward direction of the dispersal pattern from Africa of the other plant groups is more prevalent than from Southeast Asia to Africa (e.g., Yuan et al., 2005; Clayton et al., 2009; Zhou et al., 2012). However, this time frame is relatively older than the “out-of-Africa” dispersal explained for the other organisms in the Miocene (e.g., Zhou et al., 2012; Sahoo et al., 2018). In the second dispersal event, the stem age for the AF3 clade, which includes taxa from west–central Africa, is 22.9 Ma (95% HPD: 20.7–25.4 Ma) in the early Miocene (Fig. 2). This was the time before savanna vegetation expanded in west–central Africa, and wet climate and moist forests provided suitable conditions for the range expansion of *Memecylon* (Jacobs, 2004). Another divergence is inferred within the African continent at ~12.2 Ma (HPD 95%: 9.5–14.1 Ma) in the mid-Miocene and resulted in African clade 4 (Fig. 2), which includes east African taxa. Climate and environment were heterogeneous in Africa in the mid-Miocene, and aridification accelerated in most of the areas (Jacobs, 2004; Bobe, 2006). Grasslands in west-central Africa expanded, and widespread lowland tropical forest was replaced by savanna (Morley and Richards, 1993; Jacobs, 2004). At this time, forest vegetation was found in eastern Africa (Jacobs and Kabuye, 1987; Bobe, 2006). These environmental conditions might have favored dispersal of *Memecylon* from west-central Africa to east Africa.

Dispersals between Africa and Madagascar—Our ancestral range reconstruction indicated that *Memecylon* dispersed twice from Africa to Madagascar. First, an eastward LDD event of *Memecylon* occurred at ~21.3 Ma (HPD 95%: 19.1–23.8 Ma) in the early Miocene from Africa to Madagascar traversing the Mozambique

Channel. This dispersal resulted in the MA1 clade. Previous studies of African–Malagasy disjunctions in many plant groups have relied on explanations involving transoceanic LDD from Africa to Madagascar in the Miocene—for example, Melastomataceae (Renner et al., 2001), Simaroubaceae (Clayton et al., 2009), and *Uvaria* in Annonaceae (Zhou et al., 2012). In addition to bird-mediated dispersal of *Memecylon* fruits, an alternative LDD can be invoked for the African–Malagasy disjunction related to the oceanic paleo-currents in the Oligocene (which extended until early Miocene). These currents would have enabled the transport of vegetation mats from Africa to Madagascar, a process that is considered a sweepstakes mechanism (Ali and Huber, 2010). Malagasy moist tropical forests originated in the northern and eastern margins, and the island’s hyperdiverse rainforest conditions likely developed during the Oligocene and into the Miocene (Federman et al., 2015). Therefore, we speculate that the *Memecylon* radiation in Madagascar at this time might be due to high annual precipitation and the frequency of tropical cyclones in Malagasy forests (Federman et al., 2015). Although it is important to investigate habitat shifts and niche conservatism accompanying LDD, these have not been studied for *Memecylon* or other flora at this time frame.

Secondly, the MA2 lineage consists of *Memecylon* strictly from Madagascar, corresponding to *Buxifolia* in Stone (2014), and is relatively younger than clade MA1, with a stem age of 12.2 Ma (95% HPD: 9.5–14.0 Ma). Clade MA2, which is related to clade AF4, shows two equally probable ancestral areas (Malagasy and African; Fig. 3). However, this lineage is represented by only one sample in our analysis. Improved sampling of both MA2 and AF4 would provide more accurate reconstructions.

Multiple dispersals to and within South Asia—Ancestral LDD events might have permitted *Memecylon* to expand its range from Africa to South Asia about 27.6 Ma (95% HPD: 26.8–28.1 Ma). The timing of this dispersal event in the Oligocene is congruent with other hypotheses that explain the present-day distribution of a number of angiosperm groups, such as Mimosoideae (Fabaceae; Bouchenak-Khelladi et al., 2010) and *Canarium* (Burseraceae; Federman et al., 2015). The suggested LDD mechanisms for these plant groups from Africa to South Asia included birds, oceanic currents, and sweepstakes mechanisms, and sometimes involved Indian Ocean islands as “stepping stones” (Ali and Huber, 2010; Warren et al., 2010). Any of these mechanisms (or a combination of them) may have favored *Memecylon* dispersal across this route. Although climatic cooling continued in the Oligocene, tropical forests covered South Asia (Scotese, 2001). The age of *Memecylon* leaf fossils from the Indian Oligocene (Awasthi and Mehrotra, 1995; Srivastava and Mehrotra, 2009) provides evidence for this plant group occurring in South Asia. However, the accuracy of the identification of the leaf fossil, *Memecylon amplexicaulense* (Awasthi and Mehrotra, 1995), remains questionable because naming of this fossil is based on the similarity of the leaf morphology with *M. amplexicaule*

TABLE 4. Lambda parameters (λ), probability (p) and the likelihood (Ln) statistics for ER and ARD models for each character.

Character	Ln		p	λ for the favored model
	ER	ARD		
Shape of twigs	−57.54	−55.67	0.004	0.99
Shape of leaves	−59.11	−48.45	3.20E−06	0.99
Vein visibility	−61.33	−57.76	0.008	0.70
Inflorescence position	−46.09	−41.31	4.15E−05	0.69
Peduncle length	−45.68	−44.26	9.39E−05	0.87
Petal color	−37.78	−34.41	0.009	0.99

Roxb., despite the fact that leaves of *M. amplexicaule* can be confused with several other *Memecylon* taxa (Maxwell, 1980).

Memecylon elaeagni from the Seychelles is sister to a Sri Lankan clade (Fig. 1: SA1). Our divergence time analysis indicates that the stem age of *Memecylon* from the Seychelles is ~10.4 Ma (95% HPD: 8.9–13.4 Ma). The likely ancestral range of this lineage is South Asia (Fig. 3), suggesting bidirectional dispersal routes at this time, from South Asia westward to the Seychelles, and then in the reversed direction, from the Seychelles eastward to South Asia. A previously suggested dispersal through sweepstakes mechanism in the Indian Ocean (from Seychelles to South Asia) is less probable because the direction of these currents changed at the end of the Miocene (Ali and Huber, 2010). Therefore, we surmise that bird dispersal is more likely to have enabled dispersal of *Memecylon* from the Seychelles to South Asia.

Dispersals to Southeast Asia–Pacific regions—The present distributions of Southeast Asian and Pacific *Memecylon* appear to be the result of two dispersal events. One dispersal event is likely from Africa to South Asia and Southeast Asia, and then to the Pacific region (Fig. 3). This dispersal event, which initiated at ~27.6 Ma (HPD 95%: 26.8–28.1 Ma), was discussed above. Second, we propose an additional LDD event involving dispersals from South Asia to Southeast Asia, which has taken place in the Miocene at ~7.1 Ma (HPD 95%: 6.7–8.5 Ma). These two probable LDD mechanisms may have involved birds and stepping-stone routes among islands in Southeast Asia and the Pacific regions.

Character evolution

This is the first study of *Memecylon* to explore the evolution of selected morphological characters in an explicitly phylogenetic context. Ancestral state reconstruction revealed a complex history of trait evolution. A high rate of transition was observed between states for quantitative characters, such as the size of leaves and floral dimensions. However, this study provides evidence for the evolutionary changes in six selected morphological characters such as twig shape, leaf shape, prominence of leaf veins, inflorescence position, peduncle length, and petal color.

In the ancestral state reconstruction of young stems, the terete stem was favored as the ancestral state to some extent, and winged and quadrangular stems were the derived states. Terete twigs that evolved once in the African clade and once in the South Asian clade can be considered as reversals to the ancestral state. To understand the functional importance of stem shapes, detailed physiological or anatomical studies should be carried out. Several biomechanical factors correlated with stem shape have been identified in other plant groups (Speck et al., 1990; Alm eras et al., 2004), but the evolutionary importance of this trait remains poorly known across all angiosperms. Other vegetative characters, such as leaf shape and prominence of veins, were found to have functional importance in different plant groups (Nicotra et al., 2011; Schmerler et al., 2012; Sack et al., 2013), but the drivers of their evolution in *Memecylon* are not clear.

An axillary inflorescence position was reconstructed as ancestral with two independent transitions to cauliflory in the South Asian clade. The evolution of cauliflory may have been associated with an adaptation for insects to pollinate tree flowers in the lower strata of tropical forests. Cauliflory is presumably a more successful strategy than bearing flowers interspersed with leaves,

because pollinators can better visualize flowers when they are on stems than among the foliage (Warren et al., 1997). Moreover, cauliflory also correlates with improving the visibility of fruits to dispersal agents (Marshall, 1983). Cauliflory is present in other groups of Melastomataceae (e.g., Henrietteae; Penneys et al., 2010). Therefore, examination of the evolutionary patterns of cauliflory of *Memecylon* should be carried out in the context of the large Melastomataceae clade. According to species descriptions and taxonomic revisions, terminal inflorescences are uncommon in *Memecylon*, and in our analysis, this trait is found only in the South Asian and Southeast Asian clades, which evolved in the mid- to late Miocene. *Memecylon* with terminal inflorescences included in this study are found from primary and secondary forests. Terminal inflorescence seems to have evolved from the cauliflorous state, and the selective advantage of this transition is presumably enhancing the visibility of flowers and fruits to pollinators and dispersal agents in different environments or forest strata. In floral characters, the multiple, independent phylogenetic transitions among petal colors might have allowed a wide range of adaptations to various pollinators. However, the South Asian clade contained mostly blue–purple petals, except for lineages of white and pink–red petaled *Memecylon*, indicating blue–purple might have an advantage in attracting pollinators in this region. Most of the *Memecylon* scored in our study (40/61) contained short peduncles. The phylogenetic transition of short peduncle to medium and long peduncle might also have allowed adaptations to both pollinators and dispersal agents. The medium and long peduncle may enhance inflorescence visibility and can be advantageous for successful pollination. The evolutionary significance of long peduncles was studied in other plant groups (Su and Saunders, 2006; Su et al., 2008). However, limited studies on floral visitation and pollination mechanisms in *Memecylon* preclude a detailed interpretation related to the drivers of the evolution of floral characters.

We acknowledge that species included in this study are insufficient to precisely capture ancestral character states. For example, only *Mouriri* was used as outgroup from the rest of the Olisbeoideae, which may be insufficient to interpret the state of the most recent common ancestor of *Memecylon*. Additionally, all members of the east African *Memecylon* (AF2) clade have white flowers, but east African *Memecylon* with blue–purple and pink–red flowers (Stone, 2014, 2020) were not included. Similarly, the cauliflorous inflorescence is common in Malagasy *Memecylon* (Jacques-F elix, 1978; Stone, 2014), but this character state is not represented in our Malagasy species. Regarding the remaining characters in the matrix (Appendix S2), a high level of homoplasy within *Memecylon* was observed. Examples include the leaf laminar length, gland on anther connective, and calycinal crown of fruit. These characters were known to be important for traditional classifications of *Memecylon* (Maxwell, 1980; Bremer, 1983, 1988; Stone et al., 2006, 2008), but in our analyses appeared to be highly homoplasious, which highlights the complexity of trait evolution in this group. Though past studies have suggested morphological characters are conserved in *Memecylon* (e.g., Maxwell, 1980; Bremer, 1983, 1988), our study discovered only a few morphological traits that may be phylogenetically informative. Ultimately, we provide a first, broad phylogenetic perspective on the morphological evolution of this group and identify specific inflorescence and floral characters that should be included to investigate pollination and fruit dispersal syndromes in future analyses of *Memecylon*.

CONCLUSIONS

This study provides the first investigation of the evolution and historical biogeography of *Memecylon* using phylogenomic data. We identified nine major lineages in *Memecylon*, and some relationships among them are congruent with Stone (2014). *Memecylon* is shown to have originated in Africa in the Eocene. Its present-day Paleotropical distribution may have been achieved by LDD, island-hopping, and overland dispersal events. A reverse colonization event from South Asia to the Seychelles was also postulated. Diversification might also be explained by climatic oscillations in the Paleotropics.

Our study suggests that *Memecylon* harbors a number of evolutionarily derived morphological features that may contribute to the diversity within this group. For example, shape of twigs, shape of leaves, prominence of veins, inflorescence position, peduncle length, and petal color are phylogenetically informative, at least to some extent. However, most of the characters used in this study exhibited a high degree of homoplasy. To understand the origin of characters such as cauliflory and leaf venation patterns of *Memecylon*, a substantial amount of natural history data of Melastomataceae is needed. Although we are aware of our limited taxon sampling, this study still provides a first glimpse into the evolution of a selected number of *Memecylon* traits, which we hope will foster future investigations.

ACKNOWLEDGMENTS

We thank the following herbaria for accessing and depositing specimens, handling specimens, organizing the inventory, and/or destructive sampling: BKF, BNRH, BO, CAS, FLAS, FRLH, JCB, K, L, MAU, MH, MO, NSW, NU, NY, PDA, SEY, SING, US, and WII. We also thank J. Jantzen, C. Howard, and D. Samanbaddha for computational assistance; X. Shi, R. Zhou, D. Samanbaddha, D. Arifiani, S. Jeyamary, and B. Bytebier for tissue samples; the mining company PT Weda Bay Nickel Bogor, ERAMET, and I. Alawatta for providing logistical help during field collection; the botanical collecting team at Weda Bay Nickel, N. Rathnasooriya, and S. Madhumadhawa for the company in the field; and S. Manchester for fossil advice. We thank the Department of Wildlife Conservation, Department of Forest, Sri Lanka; Ezemvelo KZN Wildlife, iSimangaliso Authority, South African Department of Agriculture, Forestry, and Fisheries of South Africa; and State Forest Departments of TamilNadu, Karnataka, Kerala, Andaman, and Nicobar, India, for material collection, forest research, and export permits. This research was funded by ASPT, BSA, IAPT, UFBI, FLMNH, UF: Mildred Mason Griffith award, Davis Graduate Fellowships (to P.A.), DBT Grant Project A3: DBT/PR12720/COE/34/21/2015 (to U.K.). We are also grateful to two anonymous reviewers for comments that greatly improved the manuscript.

AUTHOR CONTRIBUTIONS

P.A. designed and carried out the project with input from N.C., W.J., and R.D.S. P.A. conducted all analyses with the assistance of N.C. and W.J. S.J. and U.K. contributed DNA samples and sequences from Indian *Memecylon*. P.A., N.C., H.K., M.M., N.P., R.D.S., and L.S.W. provided samples from the field or herbarium. P.A. wrote the manuscript with contributions from all authors.

DATA AVAILABILITY

Cleaned reads have been deposited in the National Center for Biotechnology Information (NCBI) Sequence Read Archive (PRJNA576018 and PRJNA639205). Multiple sequence alignments, partitions, phylogenetic trees, and data matrices are available from the Dryad Digital Repository: <https://doi.org/10.5061/dryad.ksn02v72w> (Amarasinghe et al., 2020).

SUPPORTING INFORMATION

Additional Supporting Information may be found online in the supporting information tab for this article.

APPENDIX S1. Sequence reference for ITS and/or ETS from GenBank.

APPENDIX S2. Morphological characters and character states used in the phylogenetic analyses.

APPENDIX S3. Voucher specimens used in examination of morphological characters.

APPENDIX S4. Variable statistics of the individual supercontig sequences used for phylogenomic analysis.

APPENDIX S5. Tanglegram comparing the nuclear tree topologies as inferred in ASTRAL-III and RAxML analyses.

APPENDIX S6. Results from PhyParts showing the amount of gene conflict at each node for the ASTRAL-III species tree.

APPENDIX S7. Quartet sampling scores for the major lineages of *Memecylon* on maximum likelihood topology.

APPENDIX S8. Maximum clade credibility tree of *Memecylon* obtained from TreePL in the context of the large clade Myrtales.

APPENDIX S9. Morphological character matrix of *Memecylon*. Only characters exhibiting unambiguous optimization are shown.

APPENDIX S10. Length of peduncles plotted for each species with minimum, maximum, and average lengths (mm).

APPENDIX S11. Maximum likelihood analysis based on concatenated ETS and ITS sequences.

LITERATURE CITED

- Aberer, A. J., D. Krompass, and A. Stamatakis. 2013. Pruning rogue taxa improves phylogenetic accuracy: an efficient algorithm and webservice. *Systematic Biology* 62: 162–166.
- Ali, J. R., and M. Huber. 2010. Mammalian biodiversity on Madagascar controlled by ocean currents. *Nature* 463: 653–656.
- Alm eras, T., E. Costes, and J. -C. Salles. 2004. Identification of biomechanical factors involved in stem shape variability between apricot tree varieties. *Annals of Botany* 93: 455–468.
- Amarasinghe, P., S. Joshi, N. Page, L. S. Wijedasa, M. Merello, H. Kathriarachchi, R. D. Stone, et al. 2020. Data from: Evolution and biogeography of *Memecylon*. *Dryad Digital Repository*. <https://doi.org/10.5061/dryad.ksn02v72w>.
- Awasthi, N., and R. C. Mehrotra. 1995. Oligocene flora from Makum Coalfield, Assam, India. *Palaebotanicist* 44: 157–188.

- Berger, B. A., R. Kriebel, D. Spalink, and K. J. Sytsma. 2016. Divergence times, historical biogeography, and shifts in speciation rates of Myrtales. *Molecular Phylogenetics and Evolution* 95: 116–136.
- Bharathi, T. R., K. K. Sampath Kumara, and H. S. Prakash. 2016. *Memecylon* species: a review of traditional information and taxonomic description. *International Journal of Pharmacy and Pharmaceutical Sciences* 8: 26–34.
- Bobe, R. 2006. The evolution of arid ecosystems in eastern Africa. *Journal of Arid Environments* 66: 564–584.
- Bouchenak-Khelladi, Y., O. Maurin, J. Hurter, and M. van der Bank. 2010. The evolutionary history and biogeography of Mimosoideae (Leguminosae): An emphasis on African acacias. *Molecular Phylogenetics and Evolution* 57: 495–508.
- Bowman, D. 1992. Monsoon Forests in North-Western Australia. II. Forest-Savanna Transitions. *Australian Journal of Botany* 40: 89–102.
- Bremer, K. 1979. Taxonomy of *Memecylon* (Melastomataceae) in Ceylon. *Opera Botanica* 50: 1–32.
- Bremer, K. 1983. Taxonomy of *Memecylon* (Melastomataceae) in Borneo. *Opera Botanica* 69: 1–47.
- Bremer, K. 1988. Melastomataceae. In M. D. Dassanayake and F. R. Fosberg [eds.], *A Revised Handbook to the Flora of Ceylon*, vol. 6, 157–240. A. A. Balkema, Rotterdam, Netherlands.
- Brown, J. W., J. F. Walker, and S. A. Smith. 2017. Phyx: phylogenetic tools for unix. *Bioinformatics* 33: 1886–1888.
- Capella-Gutiérrez, S., J. M. Silla-Martínez, and T. Gabaldón. 2009. trimAl: a tool for automated alignment trimming in large-scale phylogenetic analyses. *Bioinformatics* 25: 1972–1973.
- Clausing, G., and S. S. Renner. 2001. Molecular phylogenetics of Melastomataceae and Memecylaceae: implications for character evolution. *American Journal of Botany* 88: 486–498.
- Clayton, J. W., P. S. Soltis, and D. E. Soltis. 2009. Recent long-distance dispersal overshadows ancient biogeographical patterns in a pantropical angiosperm family (Simaroubaceae, Sapindales). *Systematic Biology* 58: 395–410.
- Collinson, M. E., and M. Pingen. 1992. Seeds of the Melastomataceae from the Miocene of Central Europe. In J. Kovar-Eder [ed.], *Palaeovegetational development in Europe*, pp. 129–139. Museum of Natural History, Vienna, Austria.
- Corner, E. J. H. 1964. *The life of plants*. Wiedenfeld and Nicolson, London, UK.
- Cowling, R. M., Ş. Procheş, and J. H. J. Vlok. 2005. On the origin of southern African subtropical thicket vegetation. *South African Journal of Botany* 71: 1–23.
- Das Das, M., D. Maity, and A. Pramanik. 2015. Typification of the name *Memecylon talbotianum* Brandis (Melastomataceae). *Phytotaxa* 203: 210.
- Drummond, A. J., M. A. Suchard, D. Xie, and A. Rambaut. 2012. Bayesian phylogenetics with BEAUti and the BEAST 1.7. *Molecular Biology and Evolution* 29: 1969–1973.
- Federman, S., A. Dornburg, A. Downie, A. F. Richard, D. C. Daly, and M. J. Donoghue. 2015. The biogeographic origin of a radiation of trees in Madagascar: implications for the assembly of a tropical forest biome. *BMC Evolutionary Biology* 15: 216.
- Gamisch, A., and H. P. Comes. 2019. Clade-age-dependent diversification under high species turnover shapes species richness disparities among tropical rainforest lineages of Bulbophyllum (Orchidaceae). *BMC Evolutionary Biology* 19: 93.
- Ganeshaiah, K. N., M. Sanjappa, R. Rao, C. Murugan, and K. N. Shivaprakash. 2019. Spatial distribution pattern of taxonomic and phylogenetic diversity of woody flora in Andaman and Nicobar Islands, India. *Forest Ecosystems* 6: 38.
- Goldenberg, R., D. S. Penneys, F. Almeda, W. S. Judd, and F. A. Michelangeli. 2008. Phylogeny of *Miconia* (Melastomataceae): Patterns of Stamen Diversification in a Megadiverse Neotropical Genus. *International Journal of Plant Sciences* 169: 963–979.
- Gonzales, R. S., N. R. Ingle, D. A. Lagunzad, and T. Nakashizuka. 2009. Seed dispersal by birds and bats in lowland Philippine forest successional area. *Biotropica* 41: 452–458.
- Gottwald, H. 1992. Hölzer aus marinen Sanden des Oberen Eozän von Helmstedt (Niedersachsen). *Palaeontographica, Abteilung B* 255: 27–103.
- Gramann, F., W. Harre, H. Kreuzer, E. R. Look, and B. Mattiat. 1975. K-Ar-ages of Eocene to Oligocene glauconitic sands from Helmstedt and Lehrte (north-western Germany). *Newsletters on Stratigraphy* 4: 71–86.
- Hickey, L. J. 1977. Stratigraphy and paleobotany of the Golden Valley Formation (Early Tertiary) of western North Dakota. *Geological Society of America Memoir* 150: 1–183.
- Jacobs, B. F. 2004. Palaeobotanical studies from tropical Africa: relevance to the evolution of forest, woodland and savannah biomes. *Philosophical Transactions of the Royal Society of London, B, Biological Sciences* 359: 1573–1583.
- Jacobs, B. F., and C. H. S. Kabuye. 1987. A middle Miocene (12.2 my old) forest in the east African rift valley, Kenya. *Journal of Human Evolution* 16: 147–155.
- Jacques-Félix, H. 1978. Les genres de Memecyleae (Melastomataceae) en Afrique, Madagascar et Mascareignes. *Adansonia, sér. 2*(18): 221–235.
- Jantzen, J. R., P. Amarasinghe, R. A. Folk, M. Reginato, F. A. Michelangeli, D. E. Soltis, N. Cellinese, and P. S. Soltis. 2020. A two-tier bioinformatic pipeline to develop probes for target capture of nuclear loci with applications in Melastomataceae. *Applications in Plant Sciences* 8: 1–14.
- Jin, G., M. P. Prabhakaran, D. Kai, S. K. Annamalai, K. D. Arunachalam, and S. Ramakrishna. 2013. Tissue engineered plant extracts as nanofibrous wound dressing. *Biomaterials* 34: 724–734.
- Johnson, M. G., E. M. Gardner, Y. Liu, R. Medina, B. Goffinet, A. J. Shaw, N. J. C. Zerega, and N. J. Wickett. 2016. HybPiper: extracting coding sequence and introns for phylogenetics from high-throughput sequencing reads using target enrichment. *Applications in Plant Sciences* 4: 1600016.
- Johnson, M. G., L. Pokorný, S. Dodsworth, L. R. Botigué, R. S. Cowan, A. Devault, W. L. Eisehardt, et al. 2019. A Universal Probe Set for Targeted Sequencing of 353 Nuclear Genes from Any Flowering Plant Designed Using k-Medoids Clustering S. Renner [ed.]. *Systematic Biology* 68: 594–606.
- Katoh, K., and D. M. Standley. 2013. MAFFT multiple sequence alignment software version 7: improvements in performance and usability. *Molecular Biology and Evolution* 30: 772–780.
- Kearse, M., R. Moir, A. Wilson, S. Stones-Havas, M. Cheung, S. Sturrock, S. Buxton, et al. 2012. Geneious Basic: An integrated and extendable desktop software platform for the organization and analysis of sequence data. *Bioinformatics* 28: 1647–1649.
- Linder, H. P. 2014. The evolution of African plant diversity. *Frontiers in Ecology and Evolution* 2: 38.
- Lucas, P. W., and R. T. Corlett. 1998. Seed dispersal by long-tailed macaques. *American Journal of Primatology* 45: 29–44.
- Marshall, A. G. 1983. Bats, flowers and fruit: evolutionary relationships in the Old World. *Botanical Journal of the Linnean Society* 20: 115–135.
- Matzke, N. J. 2013. Probabilistic historical biogeography: new models for founder-event speciation, imperfect detection, and fossils allow improved accuracy and model-testing. *Frontiers of Biogeography* 5(4): 242–248.
- Matzke, N. J. 2014. Model selection in historical biogeography reveals that founder-event speciation is a crucial process in island clades. *Systematic Biology* 63: 951–970.
- Maxwell, J. F. 1980. Revision of *Memecylon* L. (Melastomataceae) from the Malay Peninsula. *Gardens' Bulletin (Singapore)* 33: 31–150.
- Moonlight, P. W., W. H. Ardi, L. A. Padilla, K.-F. Chung, D. Fuller, D. Girmansyah, R. Hollands, et al. 2018. Dividing and conquering the fastest-growing genus: Towards a natural sectional classification of the mega-diverse genus *Begonia* (Begoniaceae). *Taxon* 67: 267–323.
- Morley, R. J., and C. W. Dick. 2003. Missing fossils, molecular clocks, and the origin of the Melastomataceae. *American Journal of Botany* 90: 1638–1644.
- Morley, R. J., and K. Richards. 1993. Gramineae cuticle: a key indicator of Late Cenozoic climatic change in the Niger Delta. *Review of Palaeobotany and Palynology* 77: 119–127.
- Nepokroeff, M., B. Bremer, and K. J. Sytsma. 1999. Reorganization of the Genus *Psychotria* and Tribe Psychotrieae (Rubiaceae) Inferred from ITS and rbcL Sequence Data. *Systematic Botany* 24: 5.
- Nayak, K. G., and P. Davidar. 2010. Pollination and breeding systems of woody plant species in tropical dry evergreen forests, southern India. *Flora (Elsevier)* 205: 745–753.

- Nicotra, A. B., A. Leigh, C. K. Boyce, C. S. Jones, K. J. Niklas, D. L. Royer, and H. Tsukaya. 2011. The evolution and functional significance of leaf shape in the angiosperms. *Functional Plant Biology* 38: 535–552.
- Pagel, M. 1999. Inferring the historical patterns of biological evolution. *Nature* 401: 877–884.
- Paradis, E., J. Claude, and K. Strimmer. 2004. APE: analyses of phylogenetics and evolution in R language. *Bioinformatics* 20: 289–290.
- Pease, J. B., J. W. Brown, J. F. Walker, C. E. Hinchliff, and S. A. Smith. 2018. Quartet Sampling distinguishes lack of support from conflicting support in the green plant tree of life. *American Journal of Botany* 105: 385–403.
- Penneys, D. S., F. A. Michelangeli, W. S. Judd, and F. Almeda. 2010. Henrietteae (Melastomataceae): A New Neotropical Berry-Fruited Tribe. *Systematic Botany* 35: 783–800.
- R Core Team. 2019. R: A language and environment for statistical computing. R Foundation for Statistical Computing, Vienna, Austria. Website: <https://www.R-project.org/>. Retrieved on 8 January 2019.
- Ree, R. H., and I. Sanmartín. 2018. Conceptual and statistical problems with the DEC+J model of founder-event speciation and its comparison with DEC via model selection. *Journal of Biogeography* 45: 741–749.
- Renner, S. S. 1993. Phylogeny and classification of the Melastomataceae and Mecynaceae. *Nordic Journal of Botany* 13: 519–540.
- Renner, S. S. 2004. Multiple Miocene Melastomataceae dispersal between Madagascar, Africa and India. *Philosophical Transactions of the Royal Society of London, B, Biological Sciences* 359: 1485–1494.
- Renner, S. S., G. Clausing, and K. Meyer. 2001. Historical biogeography of Melastomataceae: the roles of Tertiary migration and long-distance dispersal. *American Journal of Botany* 88: 1290–1300.
- Renner S.S., D. Triebel, F. Almeda, D. Stone, C. Ulloa, F.A. Michelangeli, R. Goldenberg, H. Mendoza (eds.). 2007. MEL names—a database with names of Melastomataceae. Botanische Staatssammlung, Munich, Germany. Website: <http://www.melastomataceae.net/MELnames/>. Retrieved on 3 January 2020.
- Revell, L. J. 2012. phytools: an R package for phylogenetic comparative biology (and other things). *Methods in Ecology and Evolution* 3: 217–223.
- Rueden, C. T., J. Schindelin, M. C. Hiner, B. E. DeZonia, A. E. Walter, E. T. Arena, and K. W. Eliceiri. 2017. ImageJ2: ImageJ for the next generation of scientific image data. *BMC Bioinformatics* 18: 529.
- Rutschmann, F., T. Eriksson, K. A. Salim, and E. Conti. 2007. Assessing calibration uncertainty in molecular dating: the assignment of fossils to alternative calibration points. *Systematic Biology* 56: 591–608.
- Sack, L., C. Scoffoni, G. P. John, H. Poorter, C. M. Mason, R. Mendez-Alonzo, and L. A. Donovan. 2013. How do leaf veins influence the worldwide leaf economic spectrum? Review and synthesis. *Journal of Experimental Botany* 64: 4053–4080.
- Sang, T. 2002. Utility of low-copy nuclear gene sequences in plant phylogenetics. *Critical Reviews in Biochemistry and Molecular Biology* 37: 121–147.
- Sahoo, R. K., D. J. Lohman, N. Wahlberg, C. J. Müller, O. Brattström, S. C. Collins, D. Pegg, et al. 2018. Evolution of Hypolimnas butterflies (Nymphalidae): Out-of-Africa origin and Wolbachia-mediated introgression. *Molecular Phylogenetics and Evolution* 123: 50–58.
- Sayyari, E., and S. Mirarab. 2016. Fast Coalescent-Based Computation of Local Branch Support from Quartet Frequencies. *Molecular Biology and Evolution* 33: 1654–1668.
- Schmerler, S. B., W. L. Clement, J. M. Beaulieu, D. S. Chatelet, L. Sack, M. J. Donoghue, and E. J. Edwards. 2012. Evolution of leaf form correlates with tropical–temperate transitions in *Viburnum* (Adoxaceae). *Proceedings of the Royal Society B: Biological Sciences* 279: 3905–3913.
- Scotese, C. R. 2001. Atlas of Earth History, Vol. 1. Paleogeography, PALEOMAP Project, Arlington, Texas, USA, 52 pp. Website: <http://www.scotese.com>. Retrieved on 5 March 2020.
- Sivu, A. R., M. K. R. Narayanan, N. S. Pradeep, N. A. Kumar, and A. G. Pandurangan. 2014. A new species of *Memecylon* (Melastomataceae) from the Western Ghats, India. *Edinburgh Journal of Botany* 69: 371–378.
- Smith, S. A., M. J. Moore, J. W. Brown, and Y. Yang. 2015. Analysis of phylogenomic datasets reveals conflict, concordance, and gene duplications with examples from animals and plants. *BMC Evolutionary Biology* 15: 150.
- Smith, S. A., and B. C. O'Meara. 2012. treePL: divergence time estimation using penalized likelihood for large phylogenies. *Bioinformatics* 28: 2689–2690.
- Speck, T., H.-C. Spatz, and D. Vogelhehner. 1990. Contributions to the biomechanics of plants. I. Stabilities of plant stems with strengthening elements of different cross-sections against weight and wind forces. *Botanica Acta* 103: 111–122.
- Srivastava, R., and R. C. Mehrotra. 2009. Plant fossils from Dafla Formation, west Kameng District, Arunachal Pradesh. *Palaeobotanist* 58: 33–49.
- Stamatakis, A. 2014. RAxML version 8: a tool for phylogenetic analysis and post-analysis of large phylogenies. *Bioinformatics* 30: 1312–1313.
- Stone, R. D. 2006. Phylogeny of major lineages in Melastomataceae, subfamily Olisbeioideae: utility of nuclear glyceraldehyde 3-phosphate dehydrogenase (*GapC*) gene sequences. *Systematic Botany* 31: 107–121.
- Stone, R. D. 2012. Endemism, species richness and morphological trends in Madagascan *Memecylon* (Melastomataceae). *Plant Ecology and Evolution* 145: 145–151.
- Stone, R. D. 2014. The species-rich, paleotropical genus *Memecylon* (Melastomataceae): molecular phylogenetics and revised infrageneric classification of the African species. *Taxon* 63: 539–561.
- Stone, R. D. 2020. *Memecylon afroschismaticum* sp. nov. (Melastomataceae–Olisbeioideae) endemic to the east African rift region of Rwanda, Burundi and western Tanzania. *Plant Ecology and Evolution* 153: 160–166.
- Stone, R. D. 2020. New species of *Memecylon* (Melastomataceae) from Madagascar: treasures of the TEF Herbarium. *Candollea* 75: 219–239.
- Stone, R. D., J.-P. Ghogue, and M. Cheek. 2008. Revised treatment of *Memecylon* sect. *Afzeliana* (Melastomataceae: Olisbeioideae), including three new species from Cameroon. *Key Bulletin* 63: 227–241.
- Stone, R. D., I. G. Mona, D. Styles, J. Burrows, and S. Ramdhani. 2019. Taxonomic revision of South African *Memecylon* (Melastomataceae–Olisbeioideae), including three new species. *Phytotaxa* 418: 237–257.
- Stone, R. D., G. M. Walters, and J.-P. Ghogue. 2006. *Memecylon batekeanum*, a new species from southeastern Gabon, and a note on the circumscription of *Memecylon* sect. *Mouririodea* (Melastomataceae). *Novon* 16: 276–280.
- Su, Y. C. F., G. J. D. Smith, and R. M. K. Saunders. 2008. Phylogeny of the basal angiosperm genus *Pseuduvaria* (Annonaceae) inferred from five chloroplast DNA regions, with interpretation of morphological character evolution. *Molecular Phylogenetics and Evolution* 48: 188–206.
- Su, Y. C. F., and R. M. K. Saunders. 2006. Monograph of *Pseuduvaria* (Annonaceae). *Systematic Botany Monographs* 79: 1–204.
- Swamynathan, B., and N. Parthasarathy. 2005. Community-level fruit production and dispersal modes in two tropical dry evergreen forests of peninsular India. *Tropical Biodiversity* 8(3): 159–171.
- Tanaka-Oda, A., T. Kenzo, Y. Inoue, M. Yano, K. Koba, and T. Ichie. 2015. Variation in leaf and soil $\delta^{15}\text{N}$ in diverse tree species in a lowland dipterocarp rainforest, Malaysia. *Trees* 30: 509–522.
- Thiers, B. 2020. Index Herbariorum. New York Botanical Garden, New York, USA. Website: <http://sweetgum.nybg.org/science/ih/>. Retrieved on 5 December 2019.
- van Tieghem, P. 1891. Sur la structure et les affinités des Memécylées. *Annales des Sciences Naturelles, série 7, Botanique* 13: 23–92.
- Veranso-Libalah, M. C., G. Kadereit, R. D. Stone, and T. L. P. Couvreur. 2018. Multiple shifts to open habitats in Melastomataceae (Melastomataceae) congruent with the increase of African Neogene climatic aridity. *Journal of Biogeography* 45: 1420–1431.
- van Vliet, G. J. C. M., J. Koek-Noorman, and B. J. H. ter Welle. 1981. Wood anatomy, classification and phylogeny of the Melastomataceae. *Blumea* 27: 463–473.
- Warren, B. H., D. Strasberg, J. H. Bruggemann, R. P. Prys-Jones, and C. Thébaud. 2010. Why does the biota of the Madagascar region have such a strong Asiatic flavour? *Cladistics* 26: 526–538.
- Warren, J. M., D. Z. Emamdie, and K. S. Shanmugam. 1997. Reproductive allocation and pollinator distributions in cauliflorous trees in Trinidad. *Journal of Tropical Ecology* 13: 337–345.
- Wickham, H. 2016. ggplot2: Elegant graphics for data analysis. Springer, New York, USA.

- Yin, Y., L. Jiao, M. Dong, X. Jiang, and S. Zhang. 2016. Wood resources, identification, and utilization of agarwood in China. *In* R. Mohamed [ed.], *Agarwood*, 21–38. Springer Singapore, Singapore.
- Yuan, Y.-M., S. Wohlhauser, M. Möller, J. Klackenberg, M. W. Callmander, and P. Küpfer. 2005. Phylogeny and Biogeography of *Exacum* (Gentianaceae): A Disjunctive Distribution in the Indian Ocean Basin Resulted from Long Distance Dispersal and Extensive Radiation. *Systematic Biology* 54: 21–34.
- Zhang, C., M. Rabiee, E. Sayyari, and S. Mirarab. 2018. ASTRAL-III: polynomial time species tree reconstruction from partially resolved gene trees. *BMC Bioinformatics* 19 (suppl. 6): 153.
- Zhou, L., Y. C. F. Su, D. C. Thomas, and R. M. K. Saunders. 2012. 'Out-of-Africa' dispersal of tropical floras during the Miocene climatic optimum: evidence from *Uvaria* (Annonaceae). *Journal of Biogeography* 39: 322–335.

APPENDIX 1. Accessions and voucher information for samples.

Species	Herbarium ^a	Collection number (barcode)	Collector	Country	Longitude	Latitude	NCBI accession
<i>Memecylon amplexicaule</i> Roxb.	SING	LSW44	L.S. Wijedasa, M. Niisalo & T. Webb	Singapore	103°49'02.0"E	1°21'01.8"N	SAMN12920587
<i>Memecylon australissimum</i> R.D. Stone & I.G. Mona	BNRH	He2 (2838)	R.D. Stone & P. Amarasinghe	South Africa	28°53'49.68"E	32°13'34.94"S	SAMN12920571
<i>Memecylon bachmannii</i> Engl.	NU	C3 (2833)	R.D. Stone & P. Amarasinghe	South Africa	29°43'49.61"E	31°24'04.43"S	SAMN12920555
<i>Memecylon buxifolium</i> Blume	CAS	906	R. Letsara et al.	Madagascar	44°28'37"E	17°54'41"S	SAMN15228288
<i>Memecylon caeruleum</i> Jack	SING, FLAS	SIN-TA01	P. Amarasinghe & D. Samanbaddha	Singapore	103°56'39.58"E	1°21'46.76"N	SAMN12920557
<i>Memecylon calypttratum</i> K. Bremer	MO	10626 (5010184)	J.H. Beaman, R.S. Beaman, T.E. Beaman, E.A. Christensen & P. Decker	Malaysia, Sabah	116°41'E	80.6°01'N	SAMN12920556
<i>Memecylon capitellatum</i> L.	FLAS	50999 (FLAS155002)	F.R. Fosberg et al.	Sri Lanka	81°41'32.64"E	7°42'36.72"N	SAMN12920567
<i>Memecylon clarkeanum</i> Cogn.	PDA	K53	P. Amarasinghe et al.	Sri Lanka	80°12'6.73"E	6°8'31.91"N	SAMN12920578
<i>Memecylon confusum</i> Blume	REU	827	F. Martos	Réunion	N/A	N/A	SAMN15228289
<i>Memecylon cuneatum</i> Thwaites	PDA	S10	P. Amarasinghe et al.	Sri Lanka	80°18'52.27"E	6°29'1.35"N	SAMN12920611
<i>Memecylon dasyanthum</i> Gilg & Ledermann ex Engl.	MO	947 (6147058)	X.M. van der Burgt, J. Motosh, S. Njibili & M. Elangwe	Cameroon	8°47'E	5°01'N	SAMN12920551
<i>Memecylon discolor</i> Cogn.	PDA	Z008	P. Amarasinghe et al.	Sri Lanka	80°25'29.41"E	6°25'21.23"N	SAMN12920637
<i>Memecylon elaeagni</i> Blume	SEY	3609	Bytebier & Morel	Seychelles	55.4490°E	4.6597°S	SAMN15228290
<i>Memecylon flavescens</i> Gamble	JCB	sr110	N. Page	India	77°22'8.0724"E	9°38'17.736"N	SAMN12920623
<i>Memecylon fruticosum</i> King	BKF	VC5749[LSWT17]	L.S. Wijedasa & V. Chumchumroom	Thailand	98°40'27.2"E	8°52'43.0"N	SAMN12920588
<i>Memecylon fuscescens</i> Thwaites	PDA	Z0010	P. Amarasinghe et al.	Sri Lanka	80°25'50.11"E	6°27'57.22"N	SAMN12920638
<i>Memecylon giganteum</i> Alston	PDA	K51	P. Amarasinghe et al.	Sri Lanka	80°21'38.72"E	6°15'56.53"N	SAMN12920577
<i>Memecylon gracillimum</i> Alston	PDA	D9	P. Amarasinghe et al.	Sri Lanka	80°24'36.74"E	7°37'20.11"N	SAMN12920561
<i>Memecylon grande</i> Retz	PDA	Z004	P. Amarasinghe et al.	Sri Lanka	80°25'1.91"E	6°25'16.95"N	SAMN12920635
<i>Memecylon hookeri</i> Thwaites	PDA	K46	P. Amarasinghe et al.	Sri Lanka	80°20'58.58"E	6°14'43.86"N	SAMN12920576
<i>Memecylon kollimalayanum</i> M.B.Viswan.	WII	sr114	N. Page	India	77°33'57.380"E	12°1'53.796"N	SAMN12920626
<i>Memecylon kosiense</i> R.D.Stone & I.G.Mona	NU	K5 (2823)	R.D. Stone & P. Amarasinghe	South Africa	32°81'33.92"E	27°03'76.84"S	SAMN12920580
<i>Memecylon lanceolatum</i> Blanco	US	Species Blancoanae 975 (837376)	E.D. Merrill	Philippines	N/A	N/A	SAMN12920583
<i>Memecylon lateriflorum</i> (G. Don) Bremek.	CAS	2378	J.M. Reitsma	Gabon	N/A	N/A	SAMN15228291
<i>Memecylon lawsonii</i> Gamble	WII	sr112	N. Page	India	77°18'40.921"E	8°32'54.0564"N	SAMN12920624
<i>Memecylon ligustrifolium</i> Champ. ex Benth.	FLAS	SHI XG 170701	X. Shi	China	113°15'0"E	23°30'0"N	SAMN12920585
<i>Memecylon macrophyllum</i> Thwaites	PDA	Z006	P. Amarasinghe et al.	Sri Lanka	80°31'38.61"E	6°22'53.92"N	SAMN12920636
<i>Memecylon magnifolium</i> A. Fern. & R. Fern	CAS	9525	Q. Luke	Tanzania	36°58'E	7°48'S	SAMN15228292
<i>Memecylon maxwellii</i> Wijedasa	BKF	LSWT50	L.S. Wijedasa et al.	Thailand	99°52'22.4"E	7°40'41.4"N	SAMN12920589
<i>Memecylon natalense</i> Markgr.	BNRH	B2 (15259)	J.E. Burrows et al.	South Africa	31°18'45.14"E	25°44'45.47"S	SAMN12920552

(Continued)

APPENDIX 1. (Continued)

Species	Herbarium ^a	Collection number (barcode)	Collector	Country	Longitude	Latitude	NCBI accession
<i>Memecylon orbiculare</i> Thwaites	PDA	Z0011	P. Amarasinghe et al.	Sri Lanka	80°25'36.61"E	6°25'24.53"N	SAMN12920639
<i>Memecylon pauciflorum</i> Blume	NSW	1783 (NSW924277)	D.L. Lewis	Australia	129°38'53.84"E	15°13'22.78"S	SAMN12920548
<i>Memecylon petiolatum</i> Trimen ex Alston	PDA	D11	P. Amarasinghe et al.	Sri Lanka	80°24'5.73"E	7°36'43.48"N	SAMN12920562
<i>Memecylon protrusum</i> Bakh. f.	MO	3471 (6427888)	M. Merello, I. Gushilman, I. Haris, D. Loha & B. Eser	Maluku, Halmahera	127°58'26"E	00°39'45"N	SAMN12920549
<i>Memecylon procerum</i> Thwaites	PDA	K40	P. Amarasinghe et al.	Sri Lanka	80°20'54.02"E	6°14'44.64"N	SAMN12920574
<i>Memecylon rhinophyllum</i> Thwaites	PDA	D2	P. Amarasinghe et al.	Sri Lanka	80°24'46.13"E	7°36'23.04"N	SAMN12920558
<i>Memecylon rivulare</i> K. Bremer	PDA	K11	P. Amarasinghe et al.	Sri Lanka	80°12'27.84"E	6°8'36.62"N	SAMN12920573
<i>Memecylon rostratum</i> Thwaites	PDA	D6	P. Amarasinghe et al.	Sri Lanka	80°24'42.86"E	7°36'51.33"N	SAMN12920560
<i>Memecylon schraderbergense</i> Mansf.	NSW	5797 (NSW893695)	K.D.Q. Damas, K.M. Fazang & O.K. Paul	Papua New Guinea	147°07'50.67"E	07°18'09.55"S	SAMN12920550
<i>Memecylon scolopacinum</i> Ridl.	MO	8470 (3912702)	J.H. Beaman, R.S. Beaman, P. Decker & K. Medley	Borneo	116°34'W	5°57'N	SAMN12920614
<i>Memecylon sessile</i> Benth. ex Wight & Arn.	MH	srl4	N. Page	India	76°49'53.277"E	11°21'4.5"N	SAMN12920618
<i>Memecylon soutpansbergense</i> R.D. Stone & I.G. Mona	NU	13706	J.E. Burrows et al.	South Africa	30°36'16.65"E	22°38'55.44"S	SAMN12920599
<i>Memecylon</i> spD3	PDA	D3	P. Amarasinghe et al.	Sri Lanka	80°24'31.73"E	7°37'10.21"N	SAMN12920559
<i>Memecylon</i> spK45	PDA	K45	P. Amarasinghe et al.	Sri Lanka	80°10'6.99.44"E	6°14'44.65.75"N	SAMN12920575
<i>Memecylon</i> spN8	PDA	N8	P. Amarasinghe et al.	Sri Lanka	80°20'52.82"E	6°14'46.687"N	SAMN12920597
<i>Memecylon</i> spP3	PDA	P3	P. Amarasinghe et al.	Sri Lanka	80°38'35.42"E	6°43'53.55"N	SAMN12920609
<i>Memecylon</i> sp1	N/A	srl1	S. Jeyamary	India	77°08'30.84"E	8°22'24.88"N	SAMN12920616
<i>Memecylon</i> sp3	N/A	srl3	S. Jeyamary	India	77°08'34.33"E	8°22'24.99"N	SAMN12920617
<i>Memecylon</i> sp5	FRLH	srl5	N. Page	Andaman	93°0'16.8228"E	13°9'34.1532"N	SAMN12920619
<i>Memecylon</i> sp7	FRLH	srl7	N. Page	Andaman	93°0'16.8228"E	13°9'34.1532"N	SAMN12920621
<i>Memecylon</i> sp8	WII	srl8	N. Page	India	77°23'18.334"E	8°33'54.5688"N	SAMN12920622
<i>Memecylon</i> sp16	WII	srl16	N. Page	Andaman	92°37'10.186"E	11°36'54.911"N	SAMN12920627
<i>Memecylon</i> sp18	FRLH	srl18	N. Page	Andaman	93°0'16.8228"E	13°9'34.1532"N	SAMN12920629
<i>Memecylon</i> sp. 20	WII	srl20	N. Page	India	75°49'24.445"E	11°50'10.104"N	SAMN12920630
<i>Memecylon</i> sp176	MO	176	I. Gushilman, T.J.F. Bangun & I. Haris	Maluku, Halmahera	127°58'16"E	00°32'34"N	SAMN12920544
<i>Memecylon</i> sp221	MO	221	I. Gushilman, I. Haris, B. Sau, D. Loha & B. Eser	Maluku, Halmahera	127°58'27"E	00°40'00"N	SAMN12920545
<i>Memecylon</i> sp372	MO	372 (6448626)	T.J.F. Bangun, L.A. Farivo, R. Razalamalala, S. Al Lasut & A. Yani	Maluku, Halmahera	127°58'36.87"E	00°40'01.43"N	SAMN12920546
<i>Memecylon</i> 501	MO	501	I. Gushilman, B. Fabanyo, S. Lasut & R. Mahroji	Maluku, Halmahera	127°54'48"E	00°31'34"N	SAMN12920547
<i>Memecylon sylvaticum</i> Thwaites	PDA	H6	P. Amarasinghe et al.	Sri Lanka	80°38'8.7"E	7°16'52.5"N	SAMN12920570
<i>Memecylon symplociforme</i> Merr.	US	15945 (1050204)	A.D.E. Elmer	Island of Luzon, Philippines	N/A	N/A	SAMN12920631
<i>Memecylon terminale</i> Dalzell	FRLH	srl6	N. Page	India	77°23'18.334"E	8°33'54.5688"N	SAMN12920620
<i>Memecylon torricellense</i> Lauterb.	MO	16241 (6373042)	W. Takeuchi & D. Ama	Papua New Guinea	146°56'E	6°40'S	SAMN12920632
<i>Memecylon ulopterum</i> DC.	CAS	2671	R.D. Stone et al.	Madagascar	49°12'06.7"E	18°42'13.8"S	SAMN15228293
<i>Memecylon umbellatum</i> Burm. f.	FLAS	68091404 (155093)	R.G. Cooray & N. Wirawan	Sri Lanka	80°3'3.60"E	8°24'38.16"N	SAMN12920566
<i>Memecylon umbellatum</i> Burm. f.	WII	srl13	N. Page	India	79°49'17.558"E	11°59'49.315"N	SAMN12920625
<i>Memecylon umbellatum</i> Burm. f.	WII	srl17	N. Page	India	79°49'17.554"E	11°59'49.315"N	SAMN12920628
<i>Memecylon urceolatum</i> Cogn.	PDA	D15	P. Amarasinghe et al.	Sri Lanka	80°24'5.74"E	7°36'43.42"N	SAMN12920563
<i>Memecylon varians</i> Thwaites	PDA	K56	P. Amarasinghe et al.	Sri Lanka	80°12'21.45"E	6°8'32.42"N	SAMN12920579
<i>Memecylon wightii</i> Thwaites	PDA	L1	P. Amarasinghe et al.	Sri Lanka	80°42'38.71"E	7°7'37.82"N	SAMN12920584
<i>Mouriri helleri</i> Britton	NY	2232 (962763)	J.D. Ackerman	Puerto Rico	N/A	N/A	SAMN12920610

Notes: NCBI = National Center for Biotechnology Information.
Herbarium^a = herbarium acronyms: Thiers (2020)